# The Role of Virtual Synchronous Machines in Future Power Systems: A Review and Future Trends

Baruwa Muftau, Meghdad Fazeli

*Energy Safety Research Institute, Swansea University, Swansea, SA1 8EN, UK*

**Abstract**

The large-scale integration of renewable energy sources (RESs) into the grid is reshaping the energy landscape, and can significantly impact the operation and stability of the power system. The issues stemming from the evolving energy landscape are challenging, but not insurmountable. Virtual synchronous machines (VSMs) have been proposed as a grid-friendy approach to sustainably integrate large-scale RESs into the grid. This paper provides a comprehensive review of the state-of-the-art VSM topologies proposed in literature. Further, it discusses some of the challenges which will stem from the integration of large-scale RESs into the generation mix. Thereafter, potential solutions are proposed based on insights derived from extensive academic research and demonstration projects from the energy industry.

*Keywords:* Distributed Energy Resources, Grid-connection, Inertia, Islanded, Renewable Energy Sources, Short-circuit level, Synchronous Generator, Virtual Synchronous Machine.

## Abbreviation

APL Active Power Loop

AVR Automatic Virtual Regulator

DERs Distributed Energy Resources

DSM Demand Side Management

*Corresponding author

*Email address:* 750340@swansea.ac.uk (Baruwa Muftau)

EMF Electromotive Force

EMS Energy Management Systems

ERCOT Electric Reliability Council of Texas

ESOs Electricity System Operators

ESSs Energy Storage Systems

LFO Low Frequency Oscillation

LPF Low Pass Filter

PCC Point of Common Coupling

PEC Power Electronic Converters

PEV Plug-in Electric Vehicles

PI Proportional Integral

PLL Phase Locked Loop

PSC Power Synchronization Controller

PWM Pulse Width Modulation

RESs Renewable Energy Sources

RoCoF Rate of Change of Frequency

SCL Short Circuit Level

SG Synchronous Generator

SynVC Synchronous Voltage Controller

V2G Vehicle-to-grid

V2H Vehicle-to-home

VSM Virtual Synchronous Machines

VSM0H Virtual Synchronous Machine Zero Inertia

VSYNC Virtual Synchronous Control

## 1. Introduction

The vision for a net-zero carbon economy is driving a paradigm shift in the energy landscape [1], [2]. The power system is transitioning from a centralized fossil-fuel based system to a decarbonized and decentralized smart system with energy prosumers (producers + consumers) [2–4]. It is estimated that the decarbonisation of the energy sector by 2050 will add $52 trillion to the global GDP, and a 62% reduction in air pollution related ailments [5], [6]. The National Grid is committed to decarbonizing the energy sector in compliance with the British government's directives, by replacing the conventional fossil-fueled SGs with RESs [6], [7]. RESs are often clustered with local loads, ESSs and other DERs to form a microgrid [8], [9]. The microgrid functions as a single controllable entity, which can be grid-connected via a PCC, and can operate in isolation from the grid (islanded mode) [10], [11].

Currently, most RESs operate in grid-following mode, where the grid imposes the voltage and frequency, and the RESs injects a pre-defined amount of power into the network [13], [14]. In islanded mode of operation, the microgrid must regulate the voltage and frequency within stipulated limits by maintaining power balance [15], [16]. A plethora of droop topologies have been proposed in literature to enable reliable operation of microgrids in islanded mode [17]. However, the conventional droop topologies are inertia-less and prone to transient instability [18], [19]. Moreover, most of the conventional algorithms employed on RESs in microgrids, are often designed to operate in either grid-connected or islanded modes, thus necessitating a switching mechanism during transition from grid-connected to islanded mode (and vice-versa), which can undermine the stability of the power system [20]. Reports from various ESOs have demonstrated that the increasing penetration of RESs poses significant operational and control challenges [22–24]. The British National Grid recently reported undesirable trends including declining SCLs, reduction in system inertia, dynamic voltage and frequency support, which have been directly linked to the increasing proportion of RESs in the generation mix [12], [21]. Likewise, ERCOT reported increasing voltage oscillations and declining inertia [23], [25]. Currently, the penetration of RESs on the Irish grid is capped at 65% to mitigate instability from RESs operation [26], [27]. Figs. 1 & 2 illustrates the projected trend in the SCL

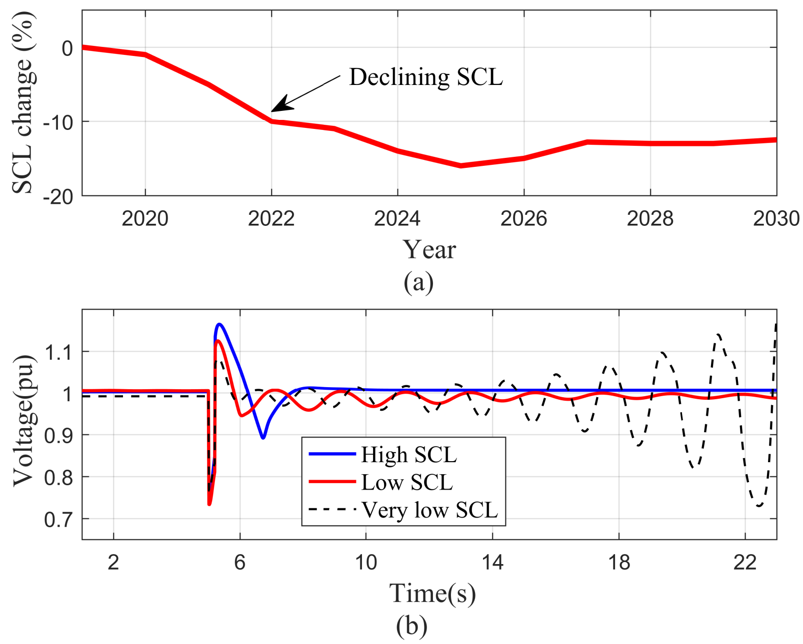


Figure 1: British National Grid SCL trend: (a) Declining SCL trend (b) Impact of declining SCL on power system dynamic performance [12].

and inertia of the British National Grid. Fig. 1(b) illustrates the dynamic response of the power system when subjected to a short circuit-fault (at t = 5s) [12]. Fig. 2(b) illustrates the frequency response of the power system when there is a sudden load change (at t = 1s) [28]. In Fig. 2(b), $\Delta f$ represents the frequency deviation from the nominal value. From Figs. 1 & 2, it is evident that the SCL and inertia, which are key indicators of the power system's strength and robustness, are on the decline; the SCL impacts the voltage stability, while the system inertia impacts the frequency stability [12], [29]. It is noted that voltage and frequency disturbances will become more intertwined with increasing RESs, such that low SCL will impact frequency stability and vice-versa [30].

For ESOs to achieve "net-zero carbon emission" [7], whilst maintaining the grid resilience and stability, RESs must employ control paradigms, which offer similar robustness as the conventional SGs [31]. Hence, the concept of grid-friendly VSMs, which mimic the dynamics of the SG have been proposed to facilitate the integration of RESs into the power system [31, 32]. Since there are a plethora of academic and industrial works on VSMs, it is necessary to collate and characterize the different design approaches, aimed to picture the future trends in the technology.

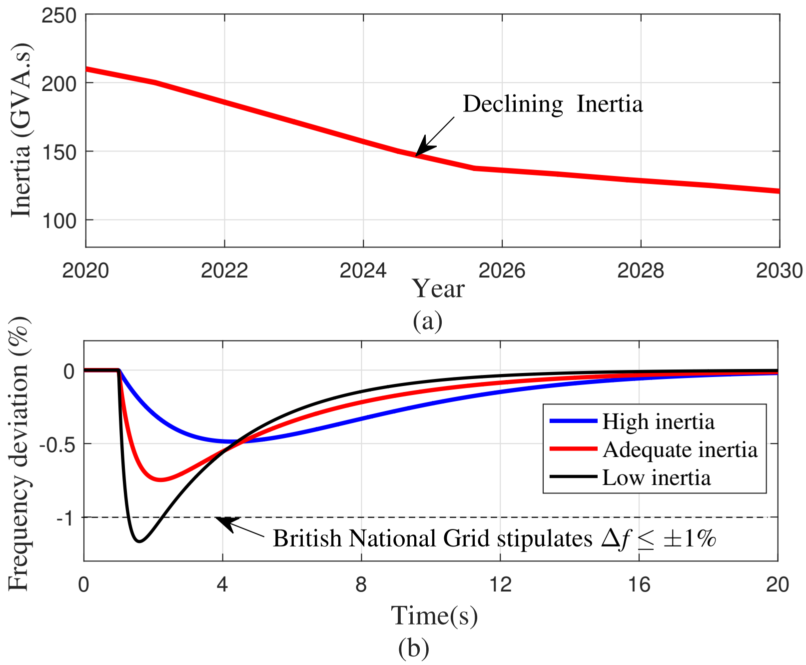


Figure 2: British National Grid inertia trend: (a) Declining inertia for "community renewables scenario" [21] (b) Illustrative frequency response for declining inertia

This paper presents a comprehensive review of the state-of the art VSM topologies, the challenges and potential solution to the integration of RESs in a decentralized and decarbonized power system. This paper is organized as follows: A comprehensive review of the VSM topologies in the literature is presented in Section II. Section III discusses some of the challenges associated with the operation of a net-zero grid, and proffers potential solutions and future research directions. Section IV concludes the paper.

## 2. Review of VSM topologies

This section provides a comprehensive review of the state-of the art VSM topologies in the literature. It describes the modelling approach of each VSM topology, the salient characteristics and the modifications required to facilitate the transition to a net-zero grid.

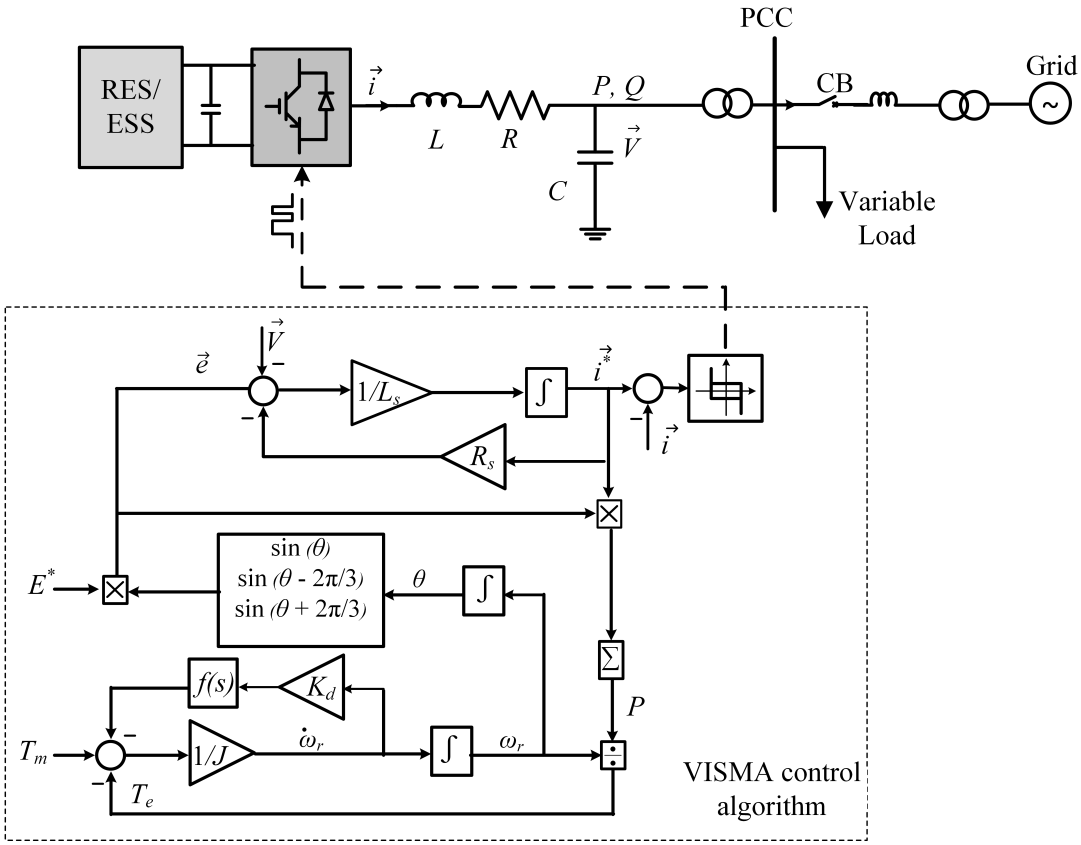


Figure 3: Topology of VISMA and the grid interface [33].

### 2.1. VISMA

The pioneer VSM algorithm was presented in [33, 34] and termed VISMA. It employs the $5^{\text{th}}$ order model of the SG to fully capture the static and dynamic characteristics of the SG. The input and output of the VISMA algorithm, are the 3-phase measured voltage $\vec{V}$ and 3-phase reference current respectively $\vec{i}^*$. A fast hysteresis controller processes $\vec{i}^*$, to derive the desired VSM operation. Unlike the conventional SG, VISMA allows bi-directional flow of active and reactive power, which caters for energy storage applications. The topology of the VISMA is illustrated in Fig. 3, and is described by (1)–(3):

$$\vec{e} = \vec{V} + \vec{i}^{*} R_s + L_s \frac{d\vec{i}^{*}}{dt} \tag{1}$$

$$\omega_r = \int \frac{T_m - T_e}{J - D_p f(s)} \tag{2}$$

$$\theta = \int \omega_r dt \tag{3}$$

Where $\vec{e} = [e_a \ e_b \ e_c]^T$ is the induced EMF in the stator winding (in *abc* frame), $R_s$ is the stator resistance and $L_s$ is the stator inductance. The measured current $\vec{i} = [i_a \ i_b \ i_c]^T$ is compared with $\vec{i}^{*} = [i_a^{*} \ i_b^{*} \ i_c^{*}]^T$ in the hysteresis controller. The notations $J$, $\omega_r$, $P$, $T_m$, $T_e$, $D_p$, $f(s)$ and $\theta$ respectively represent the moment of inertia, virtual angular frequency, active power, mechanical torque, electromagnetic torque, damping coefficient, phase compensation term and phase angle. The induced EMF reference $E^{*}$ determines the magnitude of $\vec{e}$. Although the VISMA offers considerable support for the grid-connected operation, the voltage in islanded mode is highly distorted for no-load (and presumably low-load) conditions. From Fig. 3, it is also observed that the VISMA does not employ any control for the reactive power $Q$ injected to the grid. Furthermore, when the current tracking error from the hysteresis controller is large, the VISMA does not satisfactorily replicate the desired SG dynamics [31]. Ref. [35] proposed enhancing the islanded operation of the VISMA by implementing a PWM based control. To achieve this, the input and output parameters of the VISMA were swapped such that the measured grid current and grid voltage are the input and output parameter respectively. Although this alteration improved performance in the islanded mode, the model employs a differentiator to obtain the output voltage from the current, which may lead to instability (since differentiators have a tendency to amplify noises and harmonics). Ref. [36] proposed mitigating grid harmonics by synthesizing the difference between $\vec{e}$ and $V$ by a distortion compensation factor, prior to processing by the hysteresis controller. Ref. [37] observed that neglecting the transient and sub-transient dynamics of the stator in the VISMA design resulted in undesirable transient performance. Hence, the authors [37] proposed employing an auxiliary controller in parallel with the VISMA. The auxiliary controller employs an exact replica of the VISMA but with easily adjustable parameters based on the change in operating conditions. Although this approach improves the transient performance, it increases the system complexity and significantly increases the computational burden on the digital signal processor.

*2.2. Synchronverter*

Zhong *et al.* [31], [38] proposed a VSM strategy, which offers the same dynamics as the SG from the grid point of view. Similar to the VISMA, this VSM also employs a detailed mathematical model of the SG and is termed a synchronverter. It embodies a round rotor machine (i.e. the direct and quadrature axis have the same synchronous reactance), but neglects the dampers, eddy current and iron core losses. The synchronverter is equipped with frequency and voltage droop control loops which enable parallel operation of multiple units. The frequency droop mechanism is achieved by comparing $\omega_r$ with the angular frequency reference $\omega^*$ as shown in Fig. 4. Here, $D_p$ provides both damping and $P-\omega$ droop. Unlike the VISMA, the synchronverter has a dedicated control loop for $Q$. The systems voltage is regulated by comparing the measured voltage $V$ with the reference voltage $V^*$. The error in the measured voltage is added to the reactive power control loop as shown in Fig. 4. The voltage drooping coefficient $D_q$ determines the $V-Q$ droop. The notation $\langle\cdot,\cdot\rangle$ denotes the inner product in $\mathbb{R}^3$, and the overall dynamics of the synchronverter can be represented by (4)–(9):

$$\frac{d\omega_r}{dt} = \frac{1}{J}(T_m - T_e - D_p(\omega^* - \omega_r)) \tag{4}$$

$$T_e = -M_f i_f \langle \vec{i}, \widetilde{\sin}\theta \rangle \tag{5}$$

$$E = \omega_r M_f i_f \tag{6}$$

$$e = E\widetilde{\sin}\theta \tag{7}$$

$$P = E\langle \vec{i}, \widetilde{\sin}\theta \rangle \tag{8}$$

$$Q = -E\langle \vec{i}, \widetilde{\cos}\theta \rangle \tag{9}$$

Where $P^*$, $Q^*$, $E$, $i_f$, and $M_f$ represents the reference active power, reference reactive power, amplitude of the induced EMF, field excitation current, and maximum mutual inductance between the stator windings and the field winding.

The notations $\widetilde{\sin}$ and $\widetilde{\cos}$ represent:

$$\widetilde{\sin}\theta = \begin{bmatrix} sin\theta \\ sin(\theta - \frac{2\pi}{3}) \\ sin(\theta - \frac{4\pi}{3}) \end{bmatrix}, \ \widetilde{\cos}\theta = \begin{bmatrix} cos\theta \\ cos(\theta - \frac{2\pi}{3}) \\ cos(\theta - \frac{4\pi}{3}) \end{bmatrix} \tag{10}$$

An advantage of the synchronverter over the SG, is the freedom of tuning system parameters as required (i.e. parameters such as inertia and mutual inductances are not physical) to obtain

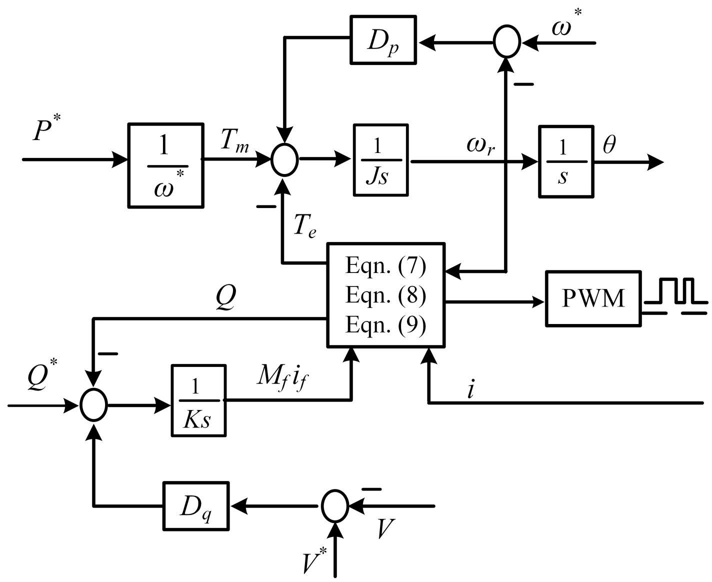


Figure 4: Control topology of the synchronverter [31].

the desired performance. However, the synchronverter also exhibits all the undesirable phenomena present in the SG including: loss of stability due to under-excitation, and hunting phenomena [31]. It is also observed that the synchronverter (see Fig. 4) employs a pure integrator to generate $\theta$. However, since the integrator accumulates the previous input states over time, this will cause a challenge in reconnection to the grid from islanding, when the integrator must be reset to achieve synchronization. This necessitates a communication from the PCC to the VSM to reset the integrator when reconnecting to the grid. Otherwise, there might be a phase shift between the VSM unit and the grid, which can even trip their operation. Several improvements on the synchronverter have been proposed in literature [38–45].

Ref. [38] augmented the structure of the synchronverter to achieve self-synchronizing capability, without the need of a PLL. The main principle of this concept is to drive the phase difference $\Delta\theta$ between $e$ from the synchronverter, and the grid voltage $V_{PCC}$ to zero, while simultaneously ensuring equal voltage magnitude (i.e. $|E| = |V_{PCC}|$). To achieve this, a synchronization mode is defined; $P$ and $Q$ are set to zero, and proportional integral (PI) controllers are used to drive $\Delta\theta$ to zero. Doing so solves the need to reset the integrator at the time of grid reconnection, at the price of creating an intermediate mode that interrupts the operation of the VSM ($P = Q = 0$). In addition, a virtual impedance is employed to drive the difference between $|V_{PCC}|$ and $|E|$ to zero.

Ref. [39] performed a stability analysis of the self-synchronizing synchronverter to facilitate optimal parameter tuning. Although, this topology [38], [39] enables self-synchronization with the grid, it adds complexity to the control paradigm. Furthermore, it does not allow seamless operation, as it necessitates a change in normal operating condition (i.e. $P$ and $Q$ must be set to zero before re-synchronization). Ref. [40] observed that, the synchronverter [31] lacks some degree of control freedom, as it is impossible to vary the response speed of the active power loop without altering the $P-\omega$ droop (which is normally fixed by the grid requirements). Hence, an additional damping correction loop was employed which enables the adjustment of the APL response without impacting the frequency droop. The authors also suggested that this technique can improve the stability of the synchronverter by reducing the active and reactive power coupling, when a fast APL response is employed.

Ref. [41] proposed a technique to limit the inrush current in the synchronverter during short-circuit fault. An inrush current detection circuit was employed to detect large inrush current during fault, thereafter the synchronverter control is switched to enable the operation of a fast hysteresis controller to limit the inrush current. Although this technique is suitable for symmetrical fault, its applicability to asymmetric fault was not discussed. Moreover, the fault detection circuit increases the system complexity. The stable operating boundary of the synchronverter was analyzed in [42], [43]. Ref. [44–46] proposed employing virtual impedance to improve the synchronverter stability, while Ref. [47] adapted the synchronverter for high voltage direct current systems. It is noted that most of the improvements for the synchronverter cannot be implemented simultaneously (e.g. the self-synchronizing control [38] cannot be simultaneously employed with the inrush current protection scheme [41]); hence, they do not provide a comprehensive solution. In addition, the complex mathematical computations required for the implementation of the control algorithm may lead to numerical instability [48].

### *2.3. ISE Lab VSM*

The ISE laboratory research group (in Osaka University, Japan) proposed a simplified model of the SG for VSM implementation [49]. This VSM has also been termed the "ISE lab" VSM in literature [48–51]. In contrast to the VISMA and synchronverter which employ the detailed dynamics of the SG, the ISE lab VSM only considers the swing equation of the SG. It employs a voltage-mode control [52], where $\theta$ and $E$ are modulated to regulate $P$ and $Q$ respectively. The

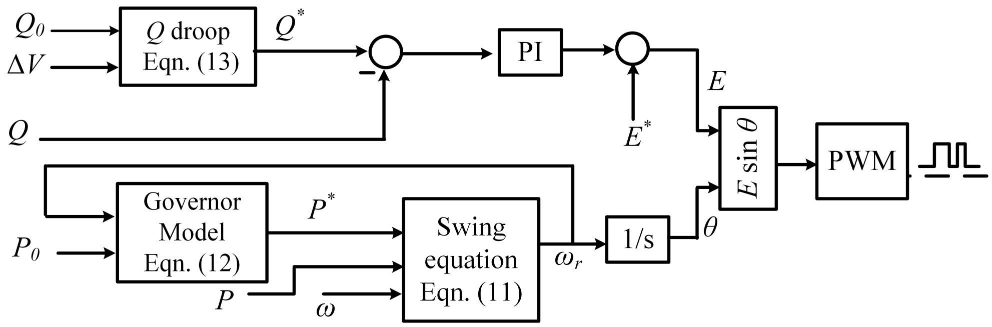


Figure 5: Topology of the ISE Lab VSM [53].

dynamics of the ISE lab VSM is represented by (11) – (13), and is illustrated in Fig. 5.

$$P^* - P = J\omega_r \frac{d\omega_r}{dt} - D\Delta\omega \tag{11}$$

$$P^* = P_0 + K_p \Delta\omega \left(\frac{1}{1 + T_d s}\right) \tag{12}$$

$$Q^* = Q_0 + K_q \Delta V \tag{13}$$

In Fig. 5, $\omega_r$ is solved from the swing equation (11) by iteration [53], while $\omega$ is the measured angular frequency obtained from a PLL. The swing equation is calculated at every control cycle to emulate the SG's inertia [48]. The governor block is a $\omega - P$ droop which regulates the reference power $P^*$ based on the angular frequency deviation $\Delta\omega$ (i.e. $\Delta\omega = \omega - \omega_r$). The governor employs a LPF with a time constant $T_d$, which emulates the mechanical delay in the governor of the SG. The ISE lab VSM was augmented with a reactive power loop in [54]. The $Q$-droop block (see Fig. 5) regulates the reactive power flow in response to voltage deviation (i.e. $\Delta V = V^* - V$). The droop gains of the active and reactive power loop are represented by $K_p$ and $K_q$ respectively. The preset active power $P_0$ and reactive power $Q_0$ are determined by the VSM rating and the ESOs requirements. Although this VSM is relatively simpler than the VISMA and synchronverter [31], [33], it suffers from reactive power sharing error and transient active power sharing error. Also, since the ISE lab VSM (see Fig. 5) employs a voltage-mode control, it has no inherent over-current protection. This can lead to undesirable and unpredictable current transients, which can damage the PEC [52]. Improvements on the ISE lab VSM were proposed in [53], [55–57].

Ref. [53] employed a virtual inductance to enhance the transient active power sharing error. Further, an inverse voltage droop ($V$–$Q$ droop) control with a common ac-bus voltage estimation was employed to achieve accurate reactive power sharing. However, if the estimated ac-bus voltage is inaccurate, the reactive power sharing will worsen. In [55], a particle swarm optimization algorithm was developed to optimally tune the system parameters to minimize phase angle deviation and achieve smooth transitions after disturbances for parallel operation of the VSM. Ref. [56], employed an alternating inertia on the VSM to damp LFOs. Ref. [57] proposed a FRT strategy for the ISE lab VSM. This was achieved by replacing the reactive power loop with a direct measurement of $V$, such that a voltage sag at PCC is directly reflected at $E$. Further, $P$ is controlled inversely proportional to $V$, while $J$ is varied in response to changes in $\omega$, to achieve satisfactory performance. However, this topology increases the VSM complexity. Further, the proposed topology is unable to inject fast-fault current as stipulated in [58].

### *2.4. VSM0H*

The VSM expert group from the National Grid (UK) proposed a zero inertia VSM control termed VSM0H [59]. The topology adopted for the VSM0H is similar to the conventional droop control. However, it does not have an inner current control loop and PI controllers. The frequency and voltage are droop regulated in proportion to the active and reactive power demand respectively. Fig. 6 illustrates the topology of the VSM0H and the dynamics of the droop block is represented by (14) and (15) below:

$$\omega_r = \omega^* + K_p(P^* - P)\left(\frac{1}{1 + T_d s}\right) \tag{14}$$

$$E = E^* + K_q(Q^* - Q) \tag{15}$$

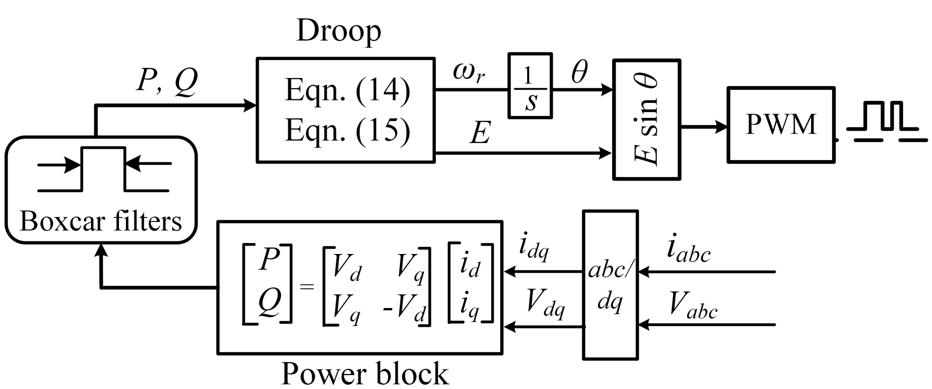


Figure 6: Control topology of the VSM0H [59].

The VSM0H is designed with a small control bandwidth (less than 50 Hz) to minimize voltage harmonics. Although the VSM0H is not equipped with synthetic inertia, it has a fast acting frequency droop slope. The capability of the VSM0H to operate in a scenario of 100% RESs penetration was demonstrated using a simplified power system model. However, an infinite bus is required to initialize the system. Similar to the synchronverter, the pure integrator on the VSM0H needs to be reset at the time of reconnecting the grid from islanding. Ref. [60] augmented the VSM0H with a phase angle correction block to enable soft-start. This was followed up by an experimental validation; however, the FRT capability was not investigated. An improvement on the VSM0H was proposed in [61] to add synthetic inertia into the VSM0H; however, this causes the system to resonate around certain frequencies (2–5 Hz). Further, since the VSM0H employs a voltage-mode control, it has no inherent over-current protection.

### *2.5. Algebraic Model of VSM*

The research team from Kawasaki Heavy Industries [62], proposed an algebraic model of the VSM, which employs the phasor representation of the SG (in steady state), while the dynamic equations of the SG are neglected. Similar to the synchronverter, the algebraic VSM also embodies a round rotor machine. It is assumed that the VSM impedance is low for a wide range of frequencies to enable smooth operation in grid and islanded mode. A major advantage of this VSM model over the previous models (e.g. synchronverter, VSM0H) is the inherent over-current protection provided by the current loop. The structure of the algebraic VSM is illustrated in Fig. 7. The dynamics of the governor (16) and AVR (17) can be represented by:

$$\omega_r = \omega^* + K_p(P^* - P)\left(\frac{1}{1+T_d s}\right) \tag{16}$$

$$E = \left[\Delta V + K_q(Q^* - Q)\left(\frac{1}{1+T_d s}\right)\right]\left(K_p + \frac{K_I}{s}\right) \tag{17}$$

The notations $E_{dq}$, $V^*_{dq}$, $V_{dq}$, $i^*_{dq}$ and $i_{dq}$ are the $dq$-axis representation of the VSM's induced EMF, reference voltage, measured voltage, reference current and measured current respectively. The relationship between $E_{dq}$, $V_{dq}$ and $i^*_{dq}$ are described in (18). The admittance $Y$ is a function of the generator's synchronous reactance $X$ and $R$. Here, $X$ is a constant, whose magnitude is independent of variations in $\omega$. The magnitude of $E$ is a function of $V^*$ and $Q^*$ from the AVR (see Fig. 7). Similarly, $\omega_r$ is a function of $P^*$ and $\omega^*$. Also, $\theta$ is obtained from the integral of the difference between the virtual angular frequency provided by the governor $\omega_r$ and $\omega$ from the PLL.

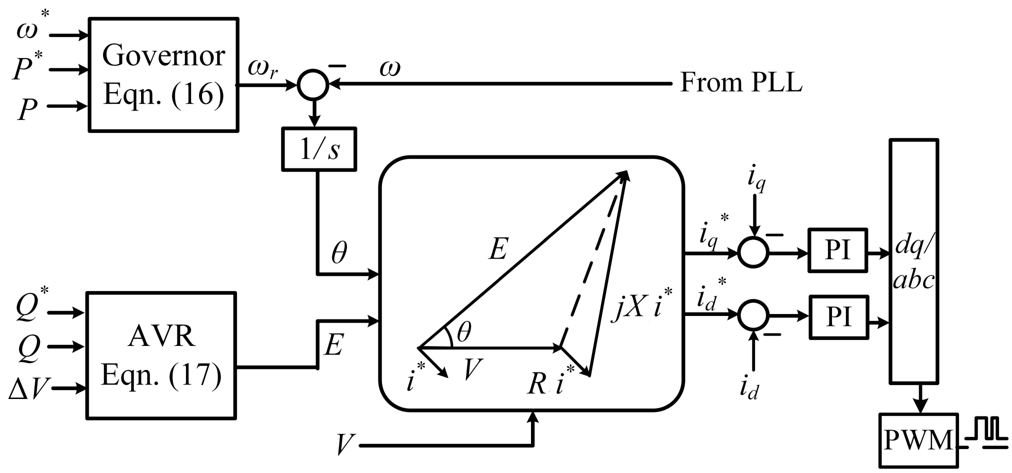


Figure 7: Control topology of the Algebraic VSM model [62].

The main drawback of this scheme is the need to switch the control topology during transition from grid to islanded mode of operation which undermines seamless operation of the system especially in cases of fault.

$$\begin{bmatrix} i_d^* \\ i_q^* \end{bmatrix} = Y \left\{ \begin{bmatrix} E_d \\ E_q \end{bmatrix} - \begin{bmatrix} V_d \\ V_q \end{bmatrix} \right\}$$
$$\begin{bmatrix} E_d \\ E_q \end{bmatrix} = E \begin{bmatrix} cos\theta \\ sin\theta \end{bmatrix}, \; Y = \frac{1}{R^2 + X^2} \begin{bmatrix} R & X \\ -X & R \end{bmatrix} \tag{18}$$

*2.6. Power synchronization controller*

Zhang et al [63] proposed a VSM which is capable of emulating the self-synchronizing capability of the SG and is termed a PSC. The active power loop (also termed as the power synchronization loop in this topology) directly controls the phase angle deviation $\Delta\theta$. The summation of the reference phase angle $\theta^*$ and $\Delta\theta$ generates $\theta$ (i.e. $\theta = \theta^* + \Delta\theta$). The dynamics of the PSC can be represented by (19):

$$\begin{aligned} \frac{d\Delta\theta}{dt} &= K_p(P^* - P) \\ \Delta E &= K_v(V^* - V)\left(\frac{1}{1 + T_d s}\right) \end{aligned} \tag{19}$$

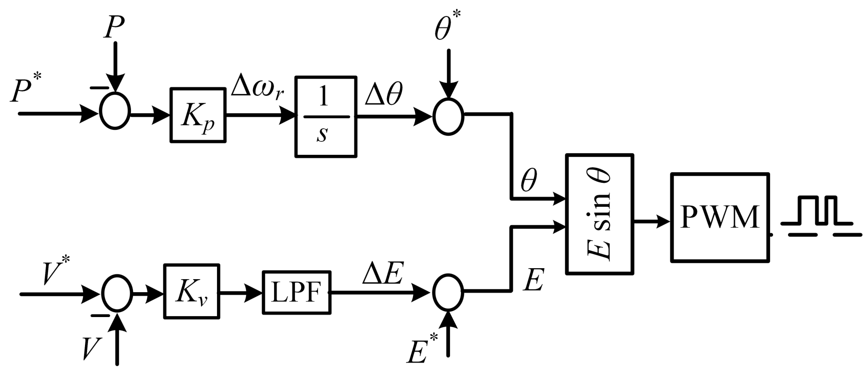


Figure 8: Power Synchronization controller [63].

The voltage control is similar to the conventional droop [17], and the voltage droop gain is represented by $K_v$. The LPF block has a time constant $T_d$. A fundamental drawback of the PSC is the absence of a current control loop, which makes the PEC vulnerable to over-current events [52]. It also suffers from large steady state error [64]. The PSC was augmented with a current controller in [65], [66] and the weak grid operation and FRT capability were demonstrated. In [67], the power loop was modified to enable independent tuning of the $P-\omega$ droop, damping and inertia of the power loop; this was achieved by employing a lead-lag compensator to emulate the swing equation of the SG. Ref. [68] proposed emulating the impedance of the SG, by augmenting the PSC with a virtual admittance. The virtual admittance improves the dynamic performance of the PSC and enables smooth transition from grid connected mode to islanded mode. However, the grid re-synchronization was not evaluated. In the aforementioned PSC topologies, grid re-synchronization will be very challenging, due to the absence of a frequency detection circuit (e.g. PLL). A presumable justification for the elimination of the frequency detection circuit will be that $f \approx 1$pu. However, in practice $f$ can vary within the nominal value stipulated in the grid code (e.g. British National Grid stipulates $\Delta f \leq \pm$ 0.01 pu) [58]. Therefore, if the grid frequency is, for example, 49.5 Hz, while the VSM reference uses the nominal 50 Hz (as there is no frequency detector), there will be a phase difference (hence a circulating current) that can interrupt the operation. Further, in islanded operation, technical and economical constraints can compel microgrid owners to employ less stringent regulation of $V$ and $f$ [9]. Hence, an attempt to re-synchronize the PEC when $V$, $f$ and $\theta$ are not within the stipulated standards will lead to large transients which can damage the PEC [69, 70]. Ref. [71] proposed a technique to enable smooth re-synchronization of the PSC to the grid. It employs a PLL at PCC to obtain the phase angle, angular frequency $\omega$ and voltage $V_{PCC}$ of the grid, while the PSC is in islanded operation. Thereafter, PI controllers are employed on the active power and voltage loop to ensure $\omega = \omega_r$ and $|E| = |V_{PCC}|$, before reconnection to the grid. A major drawback of this approach is that it also requires switch of controllers from islanded to grid-connected operation. Also, the topologies in [67], [68] employ open loop voltage control, which will impact the reactive power sharing amongst multiple systems.

### *2.7. Synchronous Voltage controller*

Ashabani et al [72] proposed a voltage based approach for SG emulation termed SynVC. Distinct from the preceeding VSM models (e.g. PSC, ISE lab VSM), where the SG emulation was realized on the power loop, the SynVC actualizes the SG emulation on the voltage loop. The overall control of the SynVC is achieved using a joint $d$-axis and joint $q$-axis control loop. The joint $d$-axis control loop regulates $i_d$, $V_d$, and provides a virtual inertia and virtual PLL. Unlike the conventional droop control [17], this topology employs an outer current loop, while the voltage loop is the inner loop. The outer current loop indirectly regulates the active power flow in the SynVC. As illustrated in Fig. 9, the error of $i_d$ is processed by the PI controller to generate $V_d^*$. Further, the deviation of $V_d$ (i.e. $\Delta V_d = V_d^* - V_d$) is processed by the virtual PLL to generate the phase angle. The LPF in the virtual PLL adds a virtual inertia and damping effect, and also attenuates PWM switching effect. The dynamics of the virtual PLL and joint $q$-axis is given by (20)–(22):

$$\theta = \int \left(\omega^* + \Delta\omega\right) \tag{20}$$

$$\Delta\omega = \left(K_p + \frac{K_I}{s}\right)\left(\frac{\Delta V_d}{1 + T_d s}\right) \tag{21}$$

$$E = (i_q^* - i_q)\left(K_p + \frac{K_I}{s}\right)\left(\frac{1}{1 + T_d s}\right) \tag{22}$$

The joint $q$-axis control loop, regulates the voltage magnitude via $i_q$. The LPF on this control loop mimics the dynamics of the $RL$ excitation circuit of the rotor in the SG. The joint $d$-axis and $q$-axis respectively perform the role of a virtual governor and virtual AVR. A major stability concern for the SynVC, is the deployment of $V_d$ instead of $V_q$ for frequency estimation. Since $V_d$ undergoes much larger excursions than $V_q$ during faults, the SynVC may be susceptible to instability or loss of synchronization post-fault. Also, although it was demonstrated that the SynVC is able to track changes in the grid variables (i.e. $V$ and $f$) in grid-connected mode, the re-synchronization

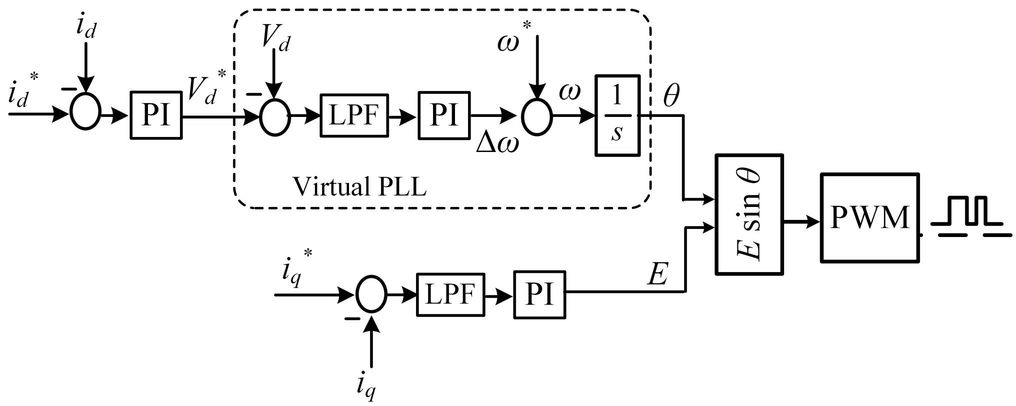


Figure 9: Topology of the synchronous voltage controller [72].

capability from an islanded mode was not investigated. An alternative to the SynVC was proposed in [64], where the SG emulation was realized on the current loop. The frequency loop directly controls the phase angle, and the reference current is synthesized from the phase angle. Although this topology has high degree of control freedom, the direct alteration of the phase angle may cause re-synchronization and stability problems [73].

### *2.8. Inducverter*

The inducverter is designed to mimic the dynamics of the induction generator. Although the inducverter is not *synchronous* in operation, it aims to achieve the core objective of the VSM i.e. mimic the desired characteristics of conventional generators to improve robustness of the grid [74]. The salient feature of the inducverter is its soft- and auto-synchronizing capability. The inducverter consists of two principal units: the current damping/synchronization unit and the core controller unit. The principal function of the current damping/synchronization unit is to accurately estimate the grid frequency and phase angle using local information, thus enabling soft- and auto-synchronization without the need of a dedicated synchronizing unit or PLL. Figure 10 illustrates the topology of the inducverter, where the angular frequency deviation $\omega_{slip}$ is estimated as a function of $i_d$ and $i_q$. Hence, $\omega_{slip}$ varies in response to variations in the output power and grid frequency

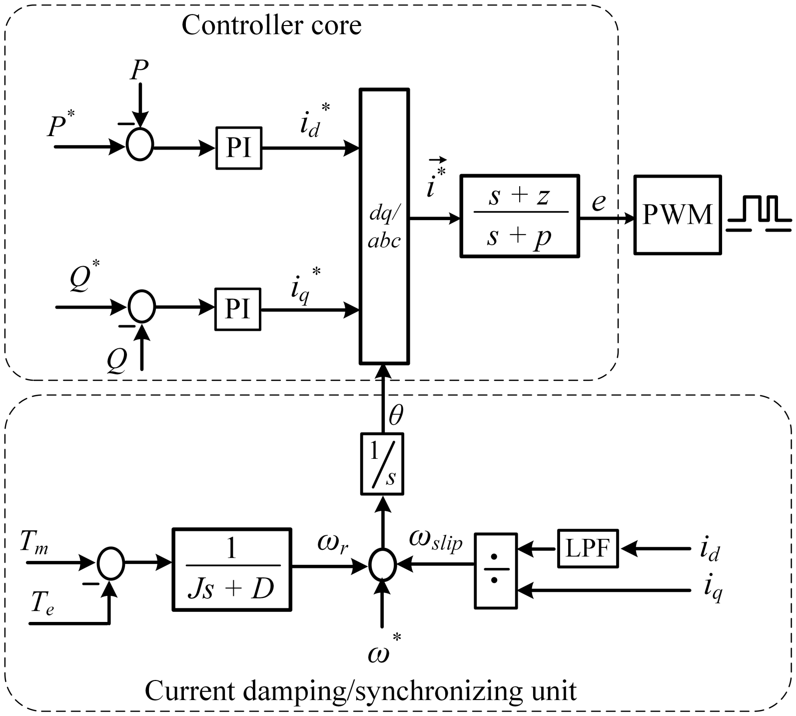


Figure 10: Topology of the Inducverter [74].

to enable auto-synchronization. The dynamics of the inducverter can be expressed by (23)–(26):

$$i_d^* = (P^* - P)\left(K_p + \frac{K_I}{s}\right) \tag{23}$$

$$i_q^* = (Q^* - Q)\left(K_p + \frac{K_I}{s}\right) \tag{24}$$

$$J\frac{d\omega_r}{dt} = T_m - T_e + D_{\omega_r} \tag{25}$$

$$\theta = \int(\omega_r + \omega_{slip} + \omega^*) \tag{26}$$

The core controller is realized using a hybrid $dq/abc$ controller as illustrated in Fig. 10. The errors of the active and reactive powers are processed via PI controllers to generate the reference current in $dq$-frame. The reference current is transformed to the equivalent $abc$ frame using the angle generated from the current damping/synchronization controller. The voltage input to the PWM is obtained from $\vec{i^*}$ using the virtual impedance. The virtual impedance is realized using an adaptive lead or lag compensator, to enhance either the transient response or steady state error respectively. In the proposed inducverter, the core controller, feeds constant amount of real and reactive powers to the grid regardless of variations in grid parameters. Although this may be advantageous for some applications, exporting constant power irrespective of voltage deviation can cause negative resistance on the grid, hence leading to instability [75]. Moreover, since the power output is kept constant regardless of grid variation, the inducverter is unable to provide fast-fault current as stipulated in [58]. From Fig. 10, it is observed that the voltage and current control are both open loop; hence, the voltage and current may exhibit undesirable transients during large disturbance [52]. Further, although the inducverter enables soft connection to the grid, its islanded operation was not investigated.

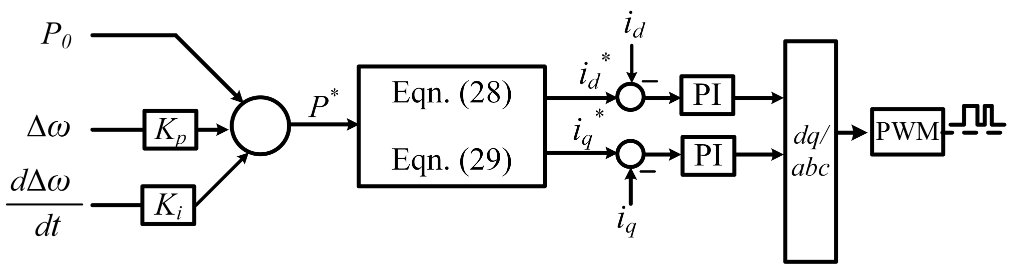


Figure 11: Control topology of VSYNC [76].

### *2.9. VSYNC*

This VSM topology was developed by the virtual synchronous control (VSYNC) research group under the 6$^{\text{th}}$ European Research Framework program [76]. VSYNC employs a PLL-based emulation of the SG [76–78]. As illustrated in Fig. 11, VSYNC employs a simple topology, which is not computationally intensive. The PLL generates $P^*$ from $\omega$ as shown in Fig. 11. This VSM topology does not implement any reactive power control and the system dynamics is described by (27)–(29).

$$P^* = P_0 + K_i \frac{d\Delta\omega}{dt} + K_p \Delta\omega \tag{27}$$

$$i_d^* = P^* \left( \frac{2V_d}{3(V_d^2 + V_q^2)} \right) \tag{28}$$

$$i_q^* = P^* \left( \frac{2V_q}{3(V_d^2 + V_q^2)} \right) \tag{29}$$

The operability of VSYNC was demonstrated via real time simulations and field tests in [79] and [80] respectively. An improvement on this topology was presented in [81], where an energy management system was implemented to enable multiple VSMs support the grid proportionally without communication. This algorithm ensures sufficient leverage for energy absorption and injection during disturbance, while preventing deep discharge or overcharge of the local ESSs. A major drawback of VSYNC is the absence of a voltage control loop. Hence, it is not applicable for islanded operations, and cannot provide dynamic voltage support to the grid.

### *2.10. Universal VSM*

Fazeli et al [73] proposed a VSM topology which enables seamless operation in all operating modes (i.e. grid-connected, islanded and during fault). A salient feature of this VSM, is that it employs a single control paradigm; hence, no switching operation is required when transiting between the different operating modes [20]. The universal VSM seamlessly operates in resistive and inductive grids and offers black-start capability. It employs the conventional *dq* current control [17], which simplifies its implementation, and provides inherent over-current protection. The control paradigm of the universal VSM topology is illustrated in Fig. 12. The dynamics of the virtual AVR and the energy management system (EMS) is represented by (30), while the dynamics of the virtual governor is given by (31):

$$i_d^* = K_v(V_d^* - V_d)\left(\frac{1}{1+T_d s}\right) + i_{dset} \tag{30}$$

$$i_q^* = K_f(f^* - f)\left(\frac{1}{1+T_d s}\right) \tag{31}$$

In Fig. 12, the notations $f_{max}$ & $f_{min}$ represents the maximum and minimum operating frequency, while $V_{d-max}$ & $V_{d-min}$ represents the maximum and minimum operating voltage stipulated by the grid code. The EMS (see Fig. 12) can be a combination of maximum power point tracking (for photovoltaic plants or wind turbines) and ESS control. The virtual AVR regulates the voltage in proportion to $i_{d-v}$, which is a function of the active power demand. The LPF on the virtual AVR provides dynamics similar to the excitation circuit of the SG, which provides damping to the VSM. The output from the virtual AVR is added to $i_{d-set}$ to obtain $i_d^*$. The virtual governor regulates the frequency in proportion to $i_q^*$, which is a function of the reactive power demand. The LPF on the virtual governor adds damping and inertial support to the VSM. It is noted that this VSM topology can also be deployed with the traditional droop $i_d - f$, $i_q - V$ as demonstrated in [82]; however, some studies have shown that the traditional droop may not yield satisfactory performance in resistive grids [83]. Ref. [3] proposed an enhanced paradigm for the universal VSM, which provides optimal support for the future grid-less power system. Here, the static LPFs in Fig. 12 were replaced with dynamic LPFs which offered superior dynamic performance. A comprehensive small-signal stability

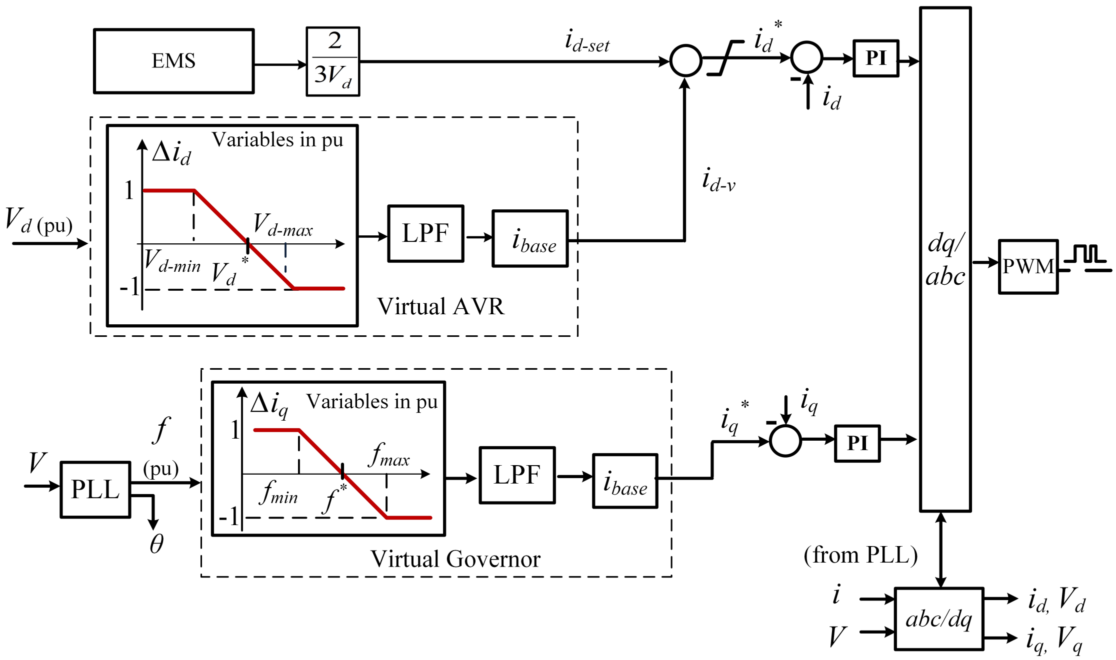


Figure 12: Control topology of the Universal VSM [73].

analysis was performed to verify the optimal value for the LPFs on the VSM. Ref. [84] employed the universal VSM as a buffer which decouples the microgrid from the main grid. The VSM droop was integrated with a dead-zone, which reduces power transmission losses by minimizing the energy exchange between the microgrid and the main grid. Similarly, studies in [85] demonstrate that this VSM topology improves the LFOs inherent in the power system. The study in [85] also corroborates the reports in [3], [84], that the power system LFOs can be eliminated by employing the universal VSM as a buffer between the SG and the grid. Although the seamless operation of the universal VSM in grid-connected and islanded modes were demonstrated, the experimental validation has not been reported.

## 3. Simulation and Discussion

It is envisaged that an ideal VSM will exhibit specific characteristics which guarantee the global stability of the power system. At the moment, no specific VSM topology has been stipulated as a recommended standard; however, some ESOs [30], [86], [87] have drafted some desirable technical

Table 1: Key features of VSM topologies

| Topology | Key features | | | | | |
|---|---|---|---|---|---|---|
| | Seamless transition between grid and islanded mode | Frequency detector (e.g. PLL) | Voltage control /AVR | Inherent over-current protection | Fault Ride-Through | Black-start capability |
| VISMA | Not investigated | None | Closed loop | Present | Not investigated | Yes |
| Synchronverter | Not realizable | Present in [38], [39] | Closed loop | Achievable in [41] | Achievable in [41] | Yes |
| ISE Lab VSM | Not investigated | None | Closed loop | None | Achievable in [57] | Yes |
| VSM0H | Not investigated | None | Closed loop | None | Not investigated | Yes |
| Algebraic VSM | Not realizable | Present | Closed loop | Present | Not investigated | Yes |
| Power Synchronization Controller | Not investigated | Present in [63] | Closed loop except [67],[68] | Present except [63] | Yes | Yes |
| Synchronous Voltage controller | Not investigated | Present | Closed loop | Present | Not investigated | Yes |
| Inducverter | Not investigated | Present | Open loop | Present | Yes | Yes |
| VSYNC VSM | Not realizable | Present | None | Present | Not investigated | Not realizable |
| Universal VSM | Yes | Present | Closed loop | Present | Yes | Yes |

Table 2: System's parameters

| Universal VSM | | |
|---|---|---|
| Parameter | Value | |
| Current Loop PI control | $K_p$ = 3e−3 | $K_i$ = 3e−2 |
| $t_f$, $t_v$ | 0.5 s, | 0.005 s |
| PLL PI control | $K_p$ = 0.015 | $K_i$ = 0.15 |
| Filter impedance | $R_f$ = 0.004 pu | $L_f$ = 0.14 pu |
| Transformer impedance | $X_L$ = 0.16 pu | |
| VSM0H | | |
| Parameter | Value | |
| Filter impedance | $R_f$ = 0.004 pu | $L_f$ = 0.14 pu |
| $t_P$, $t_Q$ | 0.05 s, | 0.05 s |
| Transformer impedance | $X_L$ = 0.16 pu | |

requirements for VSMs, which include: (i) seamless operation in grid-connected and islanded mode (ii) inherent over-current protection (iii) dynamic voltage and frequency support (iv) FRT (v) black-start capability. Based on this criteria, Table 1 provides a birds-eye view of the key features of the VSM topologies discussed in literature. Since all the VSM topologies provide frequency support, this is not highlighted in Table 1. The study in this section observes how the salient features of the VSMs can impact the grid stability for different scenarios.

To achieve this, the IEEE benchmark three-machine, nine-bus system has been implemented (Fig. 13)[88]. The VSM topologies employed in these tests are: (i) The VSM0H, which exemplifies VSMs without current control and PLL, (ii) The Universal VSM, which exemplifies VSMs with current control and PLL. The SG and network parameters are detailed in [88], [89]. The VSMs have a rating of 140 MVA, and are designed to maintain $\Delta V$ and $\Delta f$ within the nominal value [58]. The VSM parameters are detailed in Table 2. The notations $t_v$ and $t_f$ for the universal VSM represent the time constant of the damping filters on the virtual AVR and virtual governor respectively. Similarly, $t_P$ and $t_Q$ for the VSM0H represents the damping filters of the active and reactive power loop. The $V$ and $f$ are measured at bus 7 (see Fig. 13). Two test cases have been investigated:

(a) Impact of the VSM on the transient stability of the grid.

(b) Synchronization and Islanding Test

### *3.1. Impact of the VSM on the transient stability of the grid.*

According to the revised grid codes, RESs are mandated to remain connected during faults, and inject a certain amount of reactive power into the grid, thus facilitating the post-disturbance recov-

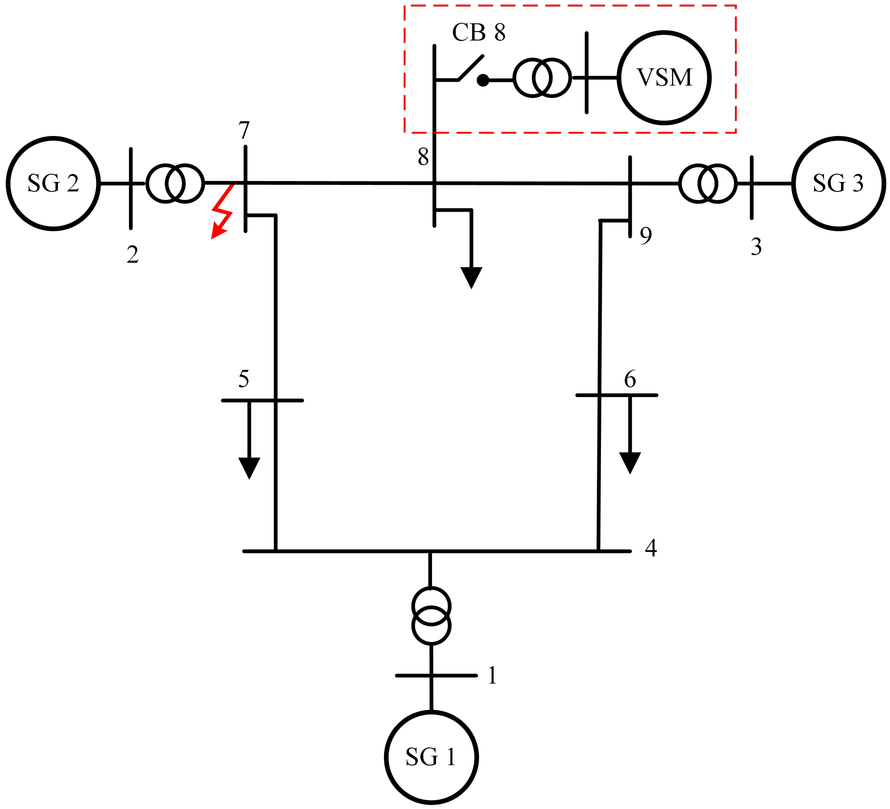


Figure 13: Modified IEEE benchmark three-machine nine-bus system [90].

ery of the power system [58], [91]. In this test, the impact of the VSM on the grid is investigated during fault. Three scenarios are observed:

(a) Response of the grid to fault without VSM.

(b) Impact of the VSM0H on the grid.

(c) Impact of the universal VSM on the grid.

A 3-phase fault is applied at bus 7, at t = 20 s. It is observed from Fig. 14(a), that the VSM0H and the universal VSM provide similar $P$ during fault, thus improving the frequency response of the system (see Fig. 14(d)). From Fig. 14(b), it is observed that during fault, the VSMs inject dynamic $Q$ into the grid as stipulated by the grid code [58]. As observed in Fig. 14(c), the injection of $Q$ improves the voltage recovery. It is noted that the VSYNC VSM (see Table. 1) will not be capable of meeting the grid requirement, due to the absence of a voltage (or AVR) loop. Similarly, the inducverter does not meet the grid requirement, as it only provides constant $Q$. Hence, it does not provide the dynamic voltage support required for the post-disturbance recovery of the grid [30], [58].

From Fig. 14 (b), it is observed that the $Q$ injected by the VSM0H is greater than 1 pu. Similarly, from Fig. 14(e), it is observed that the magnitude of the current ($I$) injected by the VSM0H is 2 pu during fault, which can damage the power electronic converter.

From Table 1, it is also observed that a number of VSM topologies (e.g. synchronverter, ISE LAB VSM) also employ the voltage-mode control as a means of mimicking the voltage source capabilities of the SG. Hence, these topologies have no inherent over-current protection, due to the absence of a current control loop. It is noted that unlike VSMs, SGs have high over-current tolerance, and are capable of injecting fast-fault currents beyond the SGs rating (e.g. $5-7$ pu) [92]. However, for VSMs with limited over-current capability, it essential to employ appropriate control loops to provide over-current protection, which is difficult (if not impossible) without a current loop.

For the universal VSM which employs a current control loop (see Fig. 14(e)), $I$ is limited to 1 pu during fault, thus protecting the power electronic converter from damage.

From the test in this sub-section (see Fig. 14), it is observed that the addition of VSMs improve the frequency response of the grid and supports the voltage recovery. However, VSMs must employ a current limiting control (e.g. with a current control loop) in order to protect the VSM from damage due to over-current.

### *3.2. Synchronization and Islanding Test*

From Table 1, it is observed that some of the topologies proposed in literature (e.g. VSM0H, ISE LAB VSM) do not employ frequency detection schemes. Hence, seamless transition from islanded to grid-connected operation may not be guaranteed.

In this test, the performance of the VSM0H is compared with the universal VSM, when synchronizing to the grid and during islanding operations. The VSMs are initially in islanded operation, at t = 15 s, the circuit breaker at bus 8 (CB 8) is closed, thus connecting the VSMs to the grid. From Fig. 15, it is observed that the universal VSM achieves a much smoother synchronization than the VSM0H. This is due to the presence of the PLL on the universal VSM, which facilitates a smooth synchronization with the grid.

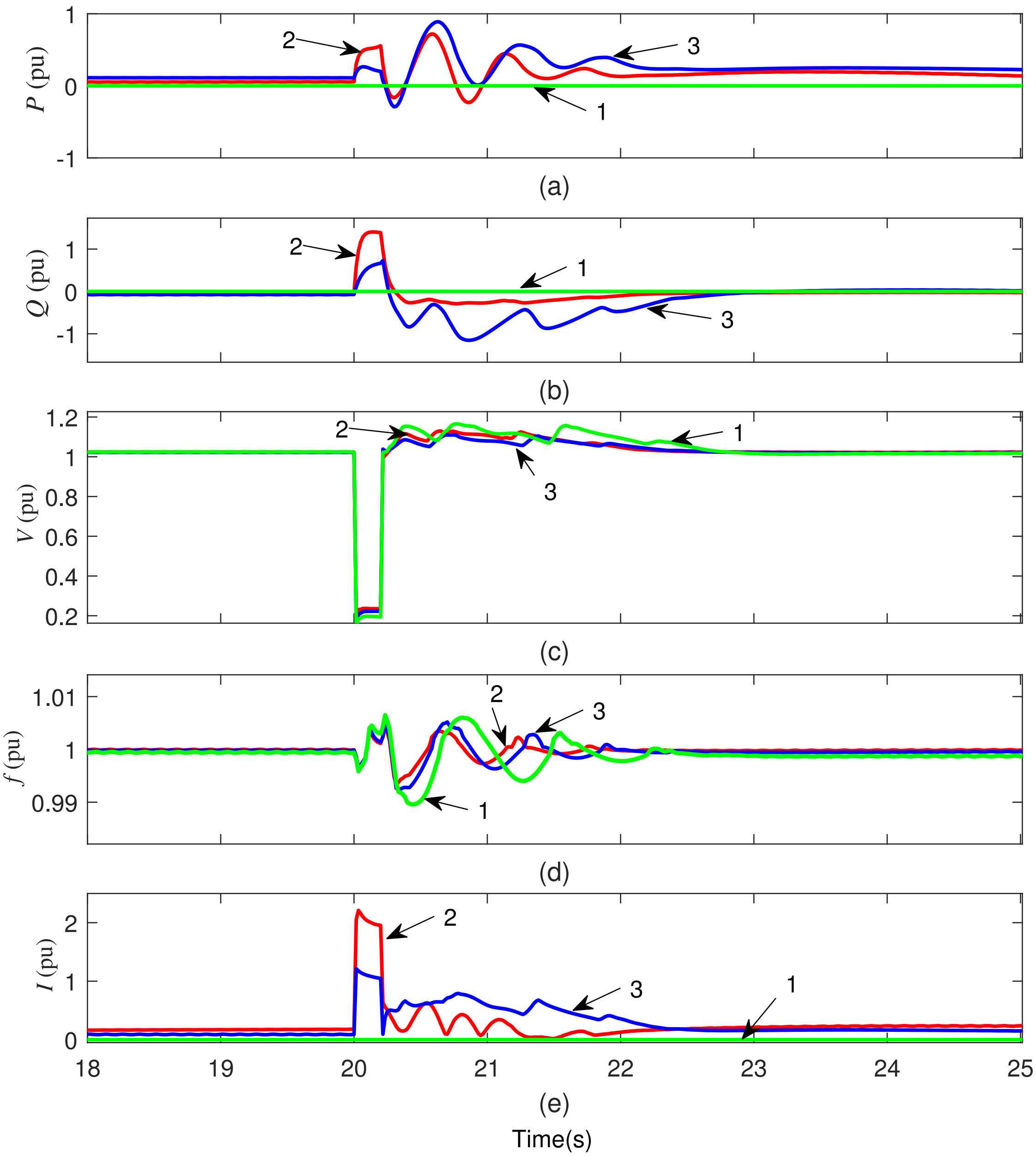


Figure 14: Impact of the VSM on the grid during faults: (a) $P$ (pu) 1-VSM0H, 2-Universal VSM, 3-no VSM. (b) $Q$ (pu) 1-VSM0H, 2-Universal VSM, 3-no VSM. (c) $V$ (pu) 1-VSM0H, 2-Universal VSM, 3-no VSM. (d) $f$ (pu) 1-VSM0H, 2-Universal VSM, 3-no VSM. (e) $I$ (pu) 1-VSM0H, 2-Universal VSM, 3-no VSM.

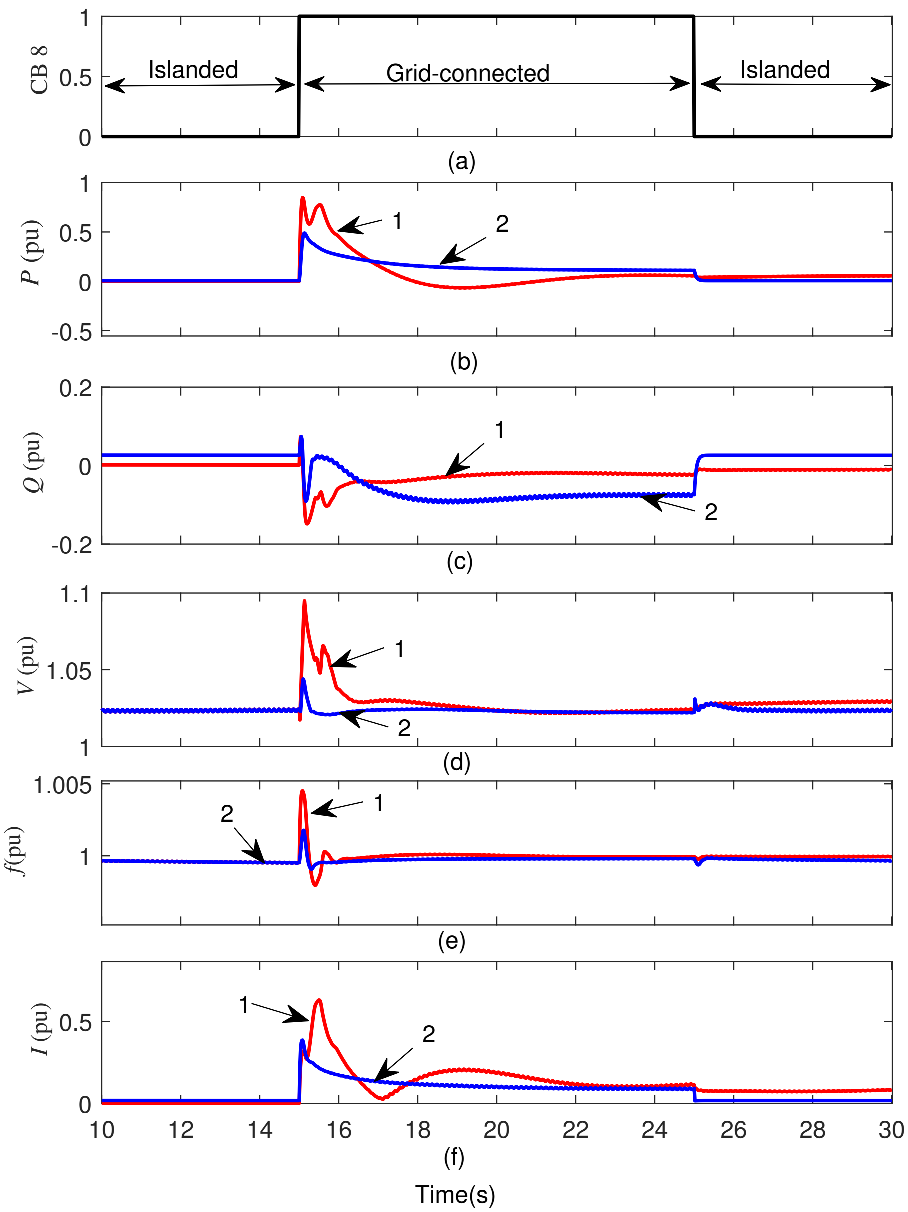


Figure 15: Grid-connected and islanded operation of the VSM:(a) CB 8. (b) $P$ (pu) 1-VSM0H, 2-Universal VSM. (c) $Q$ (pu) 1-VSM0H, 2-Universal VSM. (d) $V$ (pu) 1-VSM0H, 2-Universal VSM. (e) $f$ (pu) 1-VSM0H, 2-Universal VSM. (f) $I$ (pu) 1-VSM0H, 2-Universal VSM.

In practice, synchronism devices (e.g. phase measurement units, synchro-check relays) are often employed to match the parameters of SGs (i.e. $V$, $f$, $\theta$) prior to synchronization or parallel operation [93], [94]. Automated synchronism devices are capable of facilitating precise closure of the mains switch (i.e. at $\Delta\theta = 0^{\circ}$), thus achieving soft-synchronization [94]. Similarly, it is essential for VSMs to employ a form of frequency detection/estimation scheme to ensure soft-synchronization with the grid or adjacent microgrids. PLLs have been the standard device for synchronizing PECs to the grid [73], [74], and recent reports have demonstrated that optimally tuned PLLs can improve system stability in weak grids [95]. Also, for VSM schemes employing in-built frequency estimation schemes (e.g. synchronous voltage controller), it is essential to validate the soft-synchronization capability. It is noted that although the self-synchronizing synchronverter can achieve soft-synchronization, the transition from islanded to grid-connection operation is not seamless, as a change in operating point ($P$ and $Q = 0$) is required prior to re-connection with the grid [96].

At t = 25 s, CB 8 is opened, thus disconnecting the VSMs from the grid. As observed in Fig. 15, the islanded operation is seamless on both the VSM0H and universal VSM. This is because both VSMs have $V$ and $f$ control, thus ensuring smooth operation in islanded operation. It is assumed that VSMs capable of establishing independent regulation of $V$ and $f$ (grid-forming) can perform black-start operation [97]. From Table 1, it is observed that all the VSM topologies are capable of black-start except the VSYNC, which does not employ a voltage control loop. Hence, the VSYNC needs to be augmented with voltage control loop to enable black-start capability. The role of VSMs in the black-start of a net-zero grid will be discussed further in the next section.

Although several VSM topologies have been proposed in literature, some VSM topologies require further modifications to meet the grid requirement [58]. Table 3 summarizes the benefits and drawbacks of each of the VSMs topologies discussed above.

It is noted that VSMs employing complex algorithms (e.g. VISMA, synchronverter and inducverter) are computationally intensive, difficult to implement in real time and susceptible to numerical instability [48]. On the other hand, VSMs employing simpler models may proffer more stability to the grid [98]. At the moment, no specific VSM topology has been stipulated as a recommended standard. However, it envisaged that an ideal VSM will be capable of replicating the characteristics highlighted in this section, and thus facilitate the transition to a net-zero grid.

Table 3: Summary: Benefit and drawback of VSM topologies

| Topology | Benefit | Drawback |
|---|---|---|
| VISMA | • Detailed replication of the SG's dynamics<br>• Employs fast hysteresis control | • Prone to numerical instability<br>• Computationally intensive |
| Synchronverter | • Detailed replication of the SG's dynamics<br>• Same dynamics as SG observed from grid | • No inherent over-current protection<br>• Prone to numerical instability<br>• Computationally intensive |
| ISE VSM | • Simpler replication of SG's dynamics | • No inherent over-current protection<br>• Prone to power oscillations<br>• No frequency detection scheme |
| VSM0H | • Simple control structure<br>• Similar to the traditional droop<br>• Small control bandwidth | • No inherent over-current protection<br>• No frequency detection scheme |
| Algebraic VSM | • Phasor representation of the SG<br>• Inherent over-current protection | • Requires change of control paradigm between grid and islanded modes |
| Power synchronization controller | • Emulates self-synchronizing capability of the SG's<br>• Simple control structure | • Large steady state error<br>• Black-start requires change of algorithm |
| Synchronous voltage controller | • Emulation of the SG dynamics on voltage loop<br>• Self-synchronizing | • Potential instability during fault |

Table 3: Summary of VSM topologies (cont.d)

| Topology | Benefit | Drawback |
|---|---|---|
| Inducverter | • Replication of induction motor's dynamics<br>• soft-synchronizing and auto-synchronizing capability<br>• Employs hybrid $abc/dq$ frame<br>• Generates constant power irrespective of grid disturbance | • Open loop voltage and current control<br>• Limited fast-fault current injection<br>• Potential instability during fault |
| VSYNC VSM | • PLL emulation of the SG's swing equation<br>• Simple and easy to implement | • Susceptible to noise from frequency derivative term<br>• No islanded operation<br>• No reactive power support |
| Universal VSM | • Simple control structure<br>• Seamless operation in all operating modes<br>• Inherent over-current protection protection | • No experimental validation |

## 4. Challenges and Potential solutions

The large-scale penetration of RESs adds significant operational and technical challenges for the power system operators. This section discusses some of the challenges posed by RESs, and the potential solutions.

### *4.1. Modelling and stability analysis*

The foundation of power system analysis have been established on in-depth understanding of the SG's dynamics, associated controllers and decades of hands-on experience [99]. The increasing replacement of the well-known SGs dynamics, with the dynamics of the RESs calls for the review of the power system modelling and analysis techniques [87], [100]. In view of this, a new stability classification for microgrids has been formulated by the IEEE Power & Energy Society Task Force [10]. Ref. [101] recommended the modification of existing benchmark models to facilitate the analysis of power systems with high RESs in the generation mix. Similarly, [27] discussed the possibility of having new standards/regulations for power system variables e.g. frequency nadir and rate of change of frequency (RoCoF).

In classic power systems theory, the grid, consisting of hundreds of SGs, is often considered as an “infinite-bus” generating constant voltage and frequency; such that the dynamics of a single or small number of SGs under study will have negligible impact on the overall performance of the power system [99], [102]. However, with the decline of SGs in the generation mix, the grid may no longer behave as an infinite-bus [3], [14]. Thus, the commonly employed single machine infinite-bus model may no longer provide an insightful conclusion on the power system stability [3], [100]. As an alternative, two-machine test-bed models were employed in [85, 103, 104] to investigate the stability and dynamic performance of the power system with high RESs penetration.

Also, in the conventional power system stability studies, the grid network is commonly assumed to be quasi-static, this is because the dynamics of the SGs are much slower than the network dynamics [99], [105]. However, for RESs with fast response, the dynamic interaction of the RESs with the network will be more significant and must be evaluated to derive accurate stability reports [85], [106]. Ref. [107] also demonstrated that the quasi-static network model can provide a false conclusion of the power system stability. Hence, detailed state-space representation of the grid network will be required for accurate stability analysis of the power system [105] [106].

In the same light, the impact of the load dynamics on the system stability must be carefully considered. The proliferation of power electronic devices is changing the aggregated load dynamics [108]. In power system studies, the loads are usually represented as dynamic and/or static loads (with constant impedance, constant current and constant power (ZIP) coefficients) [102]. Studies in [75] reported that the increasing proportion of power electronics with predominantly constant power characteristics will negatively impact the system stability. Similarly, [100] employed a benchmark microgrid model, which demonstrated that the dynamic performance and stability of the power system will vary for different loads (e.g. static or dynamic loads). It is noted that modelling each load component in a system will be impractical; however, an aggregated model can be obtained by summing up the individual load characteristics of the network under study [102]. Ref. [108] carried out a comprehensive study which details the ZIP coefficients of static loads for residential, commercial and industrial sites; the resulting data from the study can be employed as a guide in modelling loads for power system stability and analysis [84].

*4.2. Demand side Management*

Large scale penetration of intermittent RESs greatly challenges the power system balance, thus necessitating greater flexibility from the demand side [109], [110]. DSM refers to a portfolio of measures (including demand side response, smart charging, vehicle-to-grid) employed to sustainably facilitate optimal and flexible energy demand from the consumer side [111], [112]. It is envisaged that the grid will transition from the traditional "load-following" operating strategy to "load-shaping" operation, where the demand side loads are flexibly managed to meet the available generating capacity [113]. Ref. [114] proposed an "energy internet" for the future grid, consisting of intelligent EMSs which facilitates the participation of prosumers in DSM. The British National Grid recently launched a stakeholder-led programme termed "power responsive", which is aimed at stimulating the participation of end users in DSM [115], [116]. Likewise, several ESOs are adopting policies for the implementation of advanced metering infrastructures, to facilitate the implementation of DSM schemes [113], [117], [118].

Demand side response is a part of DSM, which involves increasing, reducing or shifting load demand in response to signals from the ESOs [119]. It is envisaged that the future smart grid will afford ESOs direct control of consumer loads as part of the demand response scheme [109], [119]. Studies in [120, 121] have demonstrated that the systematic aggregation and modulation of demand side load can be employed to damp LFOs, thus improving power system stability. Demand side response can also minimize the impact of intermittent RESs during black-start restoration [97]. Various forecasting techniques have also been proposed in literature to facilitate efficient management of the available generation via demand response [111], [122].

PEVs and ESSs are also crucial drivers for flexible DSM [14], [123]. It is noted that some ESOs (e.g. the British National Grid) do not categorize generating sources and ESSs under demand response, but as a seperate scheme under DSM [124]. Smart deployment of ESSs can provide increased flexibility on the demand side [123]. Various ESOs envisage a significant growth in ESSs connected at the distribution level, and co-located with RESs [124]. ERCOT allows prosumers participating in DSM to deploy ESSs as "controllable load resource" when absorbing power from the grid, and as "generation resource" when injecting power back into the grid [117].

Emerging technologies including super-rapid PEV charging and inductive charging are reckoned to facilitate the adoption of PEVs [124]. The cost of PEV batteries have fallen by more than 65% since 2010 [124], and it is estimated that 100% of cars sold by 2050 will be PEVs [124], [125]. It is noted that uncontrolled integration of PEVs will detrimentally impact the distribution network [123]. Hence, PEVs must be deployed with smart charging schemes, which charge at periods of low demand and favourable tariffs [125], [126]. Further, clusters of PEVs can be exploited using "herding behavior" to provide ancilliary services to the grid via V2G schemes, and to supply domestic loads in a vehicle-to-home-scheme [123], [124]. A number of PEV manufacturers in the UK have begun test on probable V2G services [124]. Also, the Electra integrated research project group (funded by the EU) proposed a control algorithm for PEVs to provide synthetic inertia and fast frequency response for the power system[127].

A number of large-scale smart grid projects including EcoGrid EU [128], Nordhavan Energy Lab [129] and Salzburg smart grid [130], have demonstrated the operability of DSMs. Reports from various ESOs have also demonstrated that the major bottleneck in the participation of prosumers in DSM schemes are the energy policies, rather than technical barriers [117], [118]. Hence, energy markets must adopt appropriate policies and provide incentives which facilitate the engagement of prosumers, thus fostering healthy competition amongst stake-holders, and driving down the energy cost.

### *4.3. Interoperability of net-zero grid*

The power system is gearing towards net-zero operation, which implies fewer SGs in operation, and a proliferation of RESs adopting diverse control algorithms [7]. The major operational challenge arises in the interoperability of RESs with SGs, and between RESs employing diverse control paradigms. As discussed in section 2, several research works have demonstrated that VSMs are the solution to large-scale integration of RESs [31], [33]. Consequently, the British National Grid created a VSM expert group to facilitate the integration of VSMs into the grid [32]. It is expected that some architectural changes will be required to facilitate the integration of VSMs and other DERs into the grid [14], [114]. Ref.[131] suggested a partial grid-forming concept (see Fig.16(a)), where a percentage of RESs employ VSMs, while the remaining RESs employ grid-following topologies. Although, the simulated test scenarios demonstrate the feasibility of the network architecture, this architecture reduces the resilience of the grid, as grid-following converters rely on VSMs to maintain network stability. Further, the study completely neglects the operation of SGs, as it assumes a 100% converter based grid. However, it is noteworthy, that a zero carbon power system, does not totally preclude SGs from operation, as nuclear, hydro and bio-fueled power plants which are

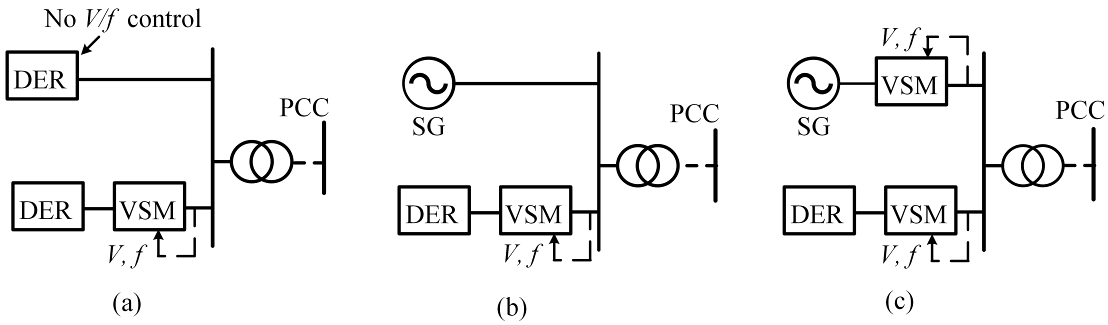


Figure 16: Simplified grid architecture (a) Partial grid-forming architecture [131] (b) VSM + SG based grid [132] (c) Grid-less architecture with decoupled SG [3].

all SG based, are clean energy sources [84]. Ref.[132], proposed that all RESs and PEC interfaced loads (e.g. motors, PEVs) are connected to the grid via VSMs (see Fig.16(b)). This will enable all the VSM controlled devices to provide inertial support to the grid, thus bolstering the grid stability [133]. However, since the SGs are still directly coupled with the grid, this topology will inherit some of the drawbacks of the conventional power system e.g. LFOs. Moreover, since SGs are very sensitive to phase angle movements, significant care must be taken to make sure that they are protected from phase angle changes in a system with a high number of VSMs. This will further complicate the reconnection and re-synchronization of SGs with the grid. Also, as stated in the Stability Pathfinder report [86], the British National Grid seeks stability products (e.g. VSMs) that can provide both inertia and SCL $\geq 1.5$ pu. These requirements are essential for the reliable operation of the power system e.g. high SCL is required for reliable operation of protection relays [12]. It is noted that while SGs can provide both inertia and SCL $\gg 1.5$ pu [92], PECs (like VSMs) have limited over-load capability and cannot supply SCL $> 1.5$ pu (unless using over-rated switches or de-loading in normal operation, which do not seem economically viable) [3]. As an alternative, Ref.[3] proposed decoupling the SGs from the grid using VSMs (see Fig. 16(c)). This eliminates the direct interaction of the SG with the grid, thus eliminating LFOs. Moreover, since only VSMs are coupled directly to the grid, a common framework can be employed, which enables VSMs operate at nominal value without requiring over-engineering or impacting operation of protection devices. Further, since SGs are decoupled from the grid, they do not have to operate at the exact grid frequency; hence, the stored kinetic energy in the rotor can be exploited to provide energy storage [3]. Also, since PECs can easily handle large phase movements, the SGs are protected from phase angle changes. This enables a fast and easy reconnection for all units.

It is noted that SGs which form the grid have virtually same dynamics, thus same mathematical equations have been used to represent all SGs regardless of the manufacturer; this facilitates power system analysis, and plug and play capability [14], [99]. At the moment, there is no unified topology for VSMs; however, the British National Grid has outlined some technical specifications and assessment criteria for VSMs [86]. As discussed in section 2, diverse control paradigms can be employed by prosumers to achieve the VSM specifications. Hence, it is essential to comprehensively validate each VSM performance, such that adding a certain VSM topology will not destabilize a hitherto stable system. The interoperability of a net-zero grid requires further research from academics and industry experts, inorder to achieve smooth transition to a zero-carbon power system. It is noted that architectural changes for a net-zero grid will also be influenced by regulatory polices and projections from cost-benefit analysis.

### *4.4. Black-Start from DERs*

Black-start is the process of restoring power to the grid after a power blackout [14] [134]. Blackouts rarely occur, and represent a worst-case scenario from the ESOs perspective [97], [135]. In the unlikely event of a blackout, the impact is often socio-economically devastating [135], [136]. For example, the 2006 European blackout affected 15 million households and led to an estimated loss of £500 million [137], [138]. Thus, adequate provisions must be in place to rapidly restore power, to minimize the impact of the blackout [134].

Conventionally, black-start has been a transmission-led approach, where large SGs re-energize transmission networks and power stations in a coordinated framework, before feeding power to consumers at the distribution level [97], [134]. However, the ongoing decarbonization of the power system and increasing proliferation of DERs necessitates a paradigm shift in the black-start process, from a transmission-led approach to a decentralized and distributed approach [97], [139].

Several research are ongoing to evaluate the feasibility of restoring power to the transmission network in a distributed-led approach [134, 140, 141]. Studies in [140] demonstrated that some VSM topologies are suitable for black-start operation. Also, some small-scale projects have been successfully deployed to demonstrate the black-start capability of DERs in a microgrid. For example, a microgrid in Schwerin, Germany, consisting of a 15 MWh battery park and gas-fired DERs successfully demonstrated black-start capability for islanded operation [142]. Similarly, a large microgrid in Fort Bragg, USA employs a variety of DERs to enable black-start capability [139], [143]. Although DERs have been deployed to black-start microgrid, it is noted that DERs have never been employed by ESOs for power restoration to the transmission network [139]. The current technical specifications for black-start operation cannot be met by DERs [97]. Hence, it is pertinent to modify the black-start frame work to enable DERs participate in the power restoration process. This will encourage participation of prosumers, thus drive down cost of black-start service, and facilitate the transition to a net-zero power system.

## 5. Conclusion

The large-scale integration of RESs significantly impacts the power system operation and stability. VSMs have been proposed as the grid-friendly approach to integrate RESs in the generation mix. This study provided a comprehensive review of the VSM topologies in literature. The IEEE three-machine nine-bus benchmark was employed to compare the performance of the VSMs. It was concluded that VSMs must employ a current-limiting strategy, and frequency detection schemes to protect the PEC from damage and ensure soft-synchronization with the grid respectively.

This paper also provided insights on some of the challenges of large-scale RESs in the generation mix, and proffered solutions to facilitate the transition to a net-zero grid. It was highlighted that, the conventional techniques for modelling and analysis of the power system will not be suitable for RESs based system. Rather, a more comprehensive framework, which considers the transmission network and load dynamics will be required for power system analysis. Also, a highly flexible demand side, with significant participation of prosumers will be required for a secure and reliable operation of a decarbonized power system.

It was recommended, that a grid-less architecture, where the SGs are decoupled from the grid, provides a common operating framework for the power system operation and control. This architecture fully exploits the inertial capability of the SGs thus improving the robustness and resilience of the power system. However, in addition to the practical implementation challenges, the cost-benefit analysis of such architecture is yet to be performed. Finally, black-start capability will be required from VSMs, as the power system becomes more decentralized and decarbonized.

It is envisaged that the discussions from this study will proffer directions for further research (in academia and the energy industry) on the operation and control of net-zero power systems.

## Acknowledgements

The support from the FLEXIS project, which is part-funded by the European Regional Development Fund through the Welsh Government, is acknowledged.

## References

[1] D. Lew, D. Bartlett, A. Groom, P. Jorgensen, J. O'Sullivan, R. Quint, B. Rew, B. Rockwell, S. Sharma, D. Stenclik, Secrets of successful integration: Operating experience with high levels of variable, inverter-based generation, IEEE Power and Energy Magazine 17 (2019). doi:10.1109/MPE.2019.2930855.

[2] National Grid, Operability Strategy Report, National Grid Warwick Technology Park, Gallows Hill, Warwick, UK., 2019. URL: https://www.nationalgrideso.com/document/159726/download, [Accessed on 11-Nov-2020].

[3] M. Fazeli, P. M. Holland, M. Baruwa, "Grid"-Less Power Systems: A Vision for Future Structure of Power Networks, IEEE Access 8 (2020). doi:10.1109/ACCESS.2020.3020455.

[4] O. Jogunola, W. Wang, B. Adebisi, Prosumers matching and least-cost energy path optimisation for peer-to-peer energy trading, IEEE Access 8 (2020) 95266–95277. doi:10.1109/ACCESS.2020.2996309.

[5] IRENA (2018), Global Energy Transformation: A roadmap to 2050, International Renewable Energy Agency, Abu Dhabi, 2018. URL: https://irena.org/-/media/Files/IRENA/Agency/Publication/2018/Apr/IRENA_Report_GET_2018.pdf?la=en&hash=9B1AF0354A2105A64CFD3C4C0E38ECCEE32AAB0C, [Accessed on 11-Nov-2020].

[6] National Grid, Towards 2030: An Electricity System Operator for Great Britain's Energy Future, National Grid Warwick Technology Park, Gallows Hill, Warwick, UK., 2019. URL: https://www.nationalgrideso.com/document/161996/download, [Accessed on 11-Nov-2020].

[7] National Grid, Future Energy Scenarios, National Grid Warwick Technology Park, Gallows Hill, Warwick, UK., 2020. URL: https://www.nationalgrideso.com/document/174541/download, [Accessed on 16-Sep-2020].

[8] R. H. Lasseter, P. Paigi, Microgrid: a conceptual solution, in: 2004 IEEE 35th Annual Power Electronics Specialists Conference (IEEE Cat. No.04CH37551), volume 6, 2004, pp. 4285–4290 Vol.6. doi:10.1109/PESC.2004.1354758.

[9] IEEE Guide for Design, Operation, and Integration of Distributed Resource Island Systems with Electric Power Systems, IEEE Std 1547.4-2011 (2011) 1–54. doi:10.1109/IEEESTD.2011.5960751.

[10] M. Farrokhabadi et al., Microgrid stability definitions, analysis, and examples, IEEE Transactions on Power Systems 35 (2020) 13–29. doi:10.1109/TPWRS.2019.2925703.

[11] Q. Jiang, M. Xue, G. Geng, Energy management of microgrid in grid-connected and stand-alone modes, IEEE Transactions on Power Systems 28 (2013) 3380–3389. doi:10.1109/TPWRS.2013.2244104.

[12] National Grid, Impact of declining short circuit levels, National Grid Warwick Technology Park, Gallows Hill, Warwick, UK., 2018. URL: https://www.nationalgrideso.com/document/135561/download, [Accessed on 12-Nov-2020].

[13] National Grid, Black Start from Non-Traditional Generation Technologies, National Grid Warwick Technology Park, Gallows Hill, Warwick, UK., 2019. URL: https://www.nationalgrideso.com/document/148201/download, [Accessed on 11-Nov-2020].

[14] B. Kroposki, B. Johnson, Y. Zhang, V. Gevorgian, P. Denholm, B. Hodge, B. Hannegan, Achieving a 100% renewable grid: Operating electric power systems with extremely high levels of variable renewable energy, IEEE Power and Energy Magazine 15 (2017) 61–73. doi:10.1109/MPE.2016.2637122.

[15] M. Fazeli, G. M. Asher, C. Klumpner, L. Yao, M. Bazargan, Novel Integration of Wind Generator-Energy Storage Systems Within Microgrids, IEEE Transactions on Smart Grid 3 (2012) 728–737. doi:10.1109/TSG.2012.2185073.

[16] M. Fazeli, G. M. Asher, C. Klumpner, L. Yao, Novel Integration of DFIG-Based Wind Generators Within Microgrids, IEEE Transactions on Energy Conversion 26 (2011) 840–850. doi:10.1109/TEC.2011.2146253.

[17] A. M. Egwebe, M. Fazeli, P. Igic, P. M. Holland, Implementation and stability study of dynamic droop in islanded microgrids, IEEE Transactions on Energy Conversion 31 (2016) 821–832. doi:10.1109/TEC.2016.2540922.

[18] L. Huang, H. Xin, Z. Wang, L. Zhang, K. Wu, J. Hu, Transient stability analysis and control design of droop-controlled voltage source converters considering current limitation, IEEE Transactions on Smart Grid 10 (2019) 578–591. doi:10.1109/TSG.2017.2749259.

[19] R. Belkacemi, S. Zarrabian, A. Babalola, R. Craven, Experimental transient stability analysis of microgrid systems: Lessons learned, in: 2015 IEEE Power Energy Society General Meeting, 2015, pp. 1–5. doi:10.1109/PESGM.2015.7286637.

[20] M. O. Baruwa, M. Fazeli, A. M. Egwebe, New control paradigm for both islanded and grid-connected operation of PMSG-based wind turbine, The Journal of Engineering (2019). doi:10.1049/joe.2018.9359.

[21] National Grid, Operating a Low Inertia System, National Grid Warwick Technology Park, Gallows Hill, Warwick, UK., 2020. URL: https://www.nationalgrideso.com/document/164586/download, [Accessed on 12-Nov-2020].

[22] ENTSO-E, High Penetration of Power Electronic Interfaced Power Sources and the Potential Contribution of Grid Forming Converters, Avenue de Cortenbergh 100, 1000 Brussels, Belgium, 2020. URL: https://eepublicdownloads.entsoe.eu/clean-documents/Publications/SOC/High_Penetration_of_Power_Electronic_Interfaced_Power_Sources_and_the_Potential_Contribution_of_Grid_Forming_Converters.pdf, [Accessed on 12-Nov-2020].

[23] J. Matevosyan, S. Sharma, S. . Huang, D. Woodfin, K. Ragsdale, S. Moorty, P. Wattles, W. Li, Proposed future ancillary services in electric reliability council of texas, in: 2015 IEEE Eindhoven PowerTech, 2015, pp. 1–6. doi:10.1109/PTC.2015.7232743.

[24] Australian Energy Market Operator, BLACK SYSTEM SOUTH AUSTRALIA 28 SEPTEMBER 2016–FINAL REPORT, Australian Energy Market Operator, 2017. URL: https://www.aemo.com.au/-/media/Files/Electricity/NEM/Market_Notices_and_Events/Power_System_Incident_Reports/2017/Integrated-Final-Report-SA-Black-System-28-September-2016.pdf, [Accessed on 12-Nov-2020].

[25] S. Huang, J. Schmall, J. Conto, J. Adams, Y. Zhang, C. Carter, Voltage control challenges on weak grids with high penetration of wind generation: ERCOT experience, in: 2012 IEEE Power and Energy Society General Meeting, 2012, pp. 1–7. doi:10.1109/PESGM.2012.6344713.

[26] M. Yu, A. J. Roscoe, A. Dyśko, C. D. Booth, R. Ierna, J. Zhu, H. Urdal, Instantaneous penetration level limits of non-synchronous devices in the british power system, IET Renewable Power Generation 11 (2017) 1211–1217. doi:10.1049/iet-rpg.2016.0352.

[27] F. Milano, F. Dörfler, G. Hug, D. J. Hill, G. Verbič, Foundations and challenges of low-inertia systems (invited paper), in: 2018 Power Systems Computation Conference (PSCC), 2018, pp. 1–25. doi:10.23919/PSCC.2018.8450880.

[28] J. Fang, H. Li, Y. Tang, F. Blaabjerg, Distributed power system virtual inertia implemented by grid-connected power converters, IEEE Transactions on Power Electronics 33 (2018) 8488–8499. doi:10.1109/TPEL.2017.2785218.

[29] R. Smith, System Operability Framework, National Grid, 2015. URL: https://www.nationalgrideso.com/document/63461/download, [Accessed on 01-Oct-2020].

[30] National Grid, Voltage and Frequency Dependency, National Grid Warwick Technology Park, Gallows Hill, Warwick, UK., 2018. URL: https://www.nationalgrideso.com/sites/eso/files/documents/SOF%20Report%20-%20Frequency%20and%20Voltage%20assessment.pdf, [Accessed on 27-Nov-2020].

[31] Q. Zhong, G. Weiss, Synchronverters: Inverters that mimic synchronous generators, IEEE Transactions on Industrial Electronics 58 (2011) 1259–1267. doi:10.1109/TIE.2010.2048839.

[32] National Grid, The potential operability benefits of Virtual Synchronous Machines and related technologies, National Grid Warwick Technology Park, Gallows Hill, Warwick, UK., 2020. URL: https://www.nationalgrideso.com/document/168376/download, [Accessed on 11-Nov-2020].

[33] Y. Chen, R. Hesse, D. Turschner, H. Beck, Improving the grid power quality using virtual synchronous machines, in: 2011 International Conference on Power Engineering, Energy and Electrical Drives, 2011, pp. 1–6. doi:10.1109/PowerEng.2011.6036498.

[34] H. Beck, R. Hesse, Virtual synchronous machine, in: 2007 9th International Conference on Electrical Power Quality and Utilisation, 2007, pp. 1–6. doi:10.1109/EPQU.2007.4424220.

[35] H. Beck, R. Hesse, Comparison of methods for implementing virtual synchronous machine on inverters, in: 2012 International Conference on Renewable Energies and Power Quality (ICREPQ'12), 2012, pp. 1–6.

[36] R. Hesse, D. Turschner, H.-P. Beck, Micro grid stabilization using the virtual synchronous machine (VISMA), Renewable energy and power quality journal 1 (2009) 676–681.

[37] Y. Chen, R. Hesse, D. Turschner, H.-P. Beck, Dynamic properties of the virtual synchronous machine (visma), Renewable energy and power quality journal (2011) 755–759.

[38] Q.-C. Zhong, P.-L. Nguyen, Z. Ma, W. Sheng, Self-synchronized synchronverters: Inverters without a dedicated synchronization unit, IEEE Transactions on Power Electronics 29 (2014) 617–630. doi:10.1109/TPEL.2013.2258684.

[39] S. Dong, J. Jiang, Y. C. Chen, Analysis of synchronverter self-synchronization dynamics to facilitate parameter tuning, IEEE Transactions on Energy Conversion 35 (2020) 11–23. doi:10.1109/TEC.2019.2945958.

[40] S. Dong, Y. C. Chen, Adjusting synchronverter dynamic response speed via damping correction loop, IEEE Transactions on Energy Conversion 32 (2017) 608–619. doi:10.1109/TEC.2016.2645450.

[41] Z. Shuai, W. Huang, C. Shen, J. Ge, Z. J. Shen, Characteristics and restraining method of fast transient inrush fault currents in synchronverters, IEEE Transactions on Industrial Electronics 64 (2017) 7487–7497. doi:10.1109/TIE.2017.2652362.

[42] Z. Shuai, Y. Hu, Y. Peng, C. Tu, Z. J. Shen, Dynamic stability analysis of synchronverter-dominated microgrid based on bifurcation theory, IEEE Transactions on Industrial Electronics 64 (2017) 7467–7477. doi:10.1109/TIE.2017.2652387.

[43] Q. Zhong, G. C. Konstantopoulos, B. Ren, M. Krstic, Improved synchronverters with bounded frequency and voltage for smart grid integration, IEEE Transactions on Smart Grid 9 (2018) 786–796. doi:10.1109/TSG.2016.2565663.

[44] P. Piya, M. Karimi-Ghartemani, A stability analysis and efficiency improvement of synchronverter, in: 2016 IEEE Applied Power Electronics Conference and Exposition (APEC), 2016, pp. 3165–3171. doi:10.1109/APEC.2016.7468317.

[45] R. Rosso, S. Engelken, M. Liserre, Robust stability analysis of synchronverters operating in parallel, IEEE Transactions on Power Electronics 34 (2019) 11309–11319. doi:10.1109/TPEL.2019.2896707.

[46] V. Natarajan, G. Weiss, Synchronverters with better stability due to virtual inductors, virtual capacitors, and anti-windup, IEEE Transactions on Industrial Electronics 64 (2017) 5994–6004. doi:10.1109/TIE.2017.2674611.

[47] R. Aouini, B. Marinescu, K. Ben Kilani, M. Elleuch, Synchronverter-Based Emulation and Control of HVDC Transmission, IEEE Transactions on Power Systems 31 (2016) 278–286. doi:10.1109/TPWRS.2015.2389822.

[48] U. Tamrakar, D. Shrestha, M. Maharjan, B. P. Bhattarai, T. M. Hansen, R. Tonkoski, Virtual inertia: Current trends and future directions, Applied Sciences 7 (2017). doi:10.3390/app7070654.

[49] K. Sakimoto, Y. Miura, T. Ise, Stabilization of a power system with a distributed generator by a virtual synchronous generator function, in: 8th International Conference on Power Electronics - ECCE Asia, 2011, pp. 1498–1505. doi:10.1109/ICPE.2011.5944492.

[50] H. Bevrani, T. Ise, Y. Miura, Virtual synchronous generators: A survey and new perspectives, International Journal of Electrical Power and Energy Systems 54 (2014) 244 – 254. doi:https://doi.org/10.1016/j.ijepes.2013.07.009.

[51] K. M. Cheema, A comprehensive review of virtual synchronous generator, International Journal of Electrical Power and Energy Systems 120 (2020) 106006. doi:https://doi.org/10.1016/j.ijepes.2020.106006.

[52] A. Yazdani, R. Iravani, Voltage-Sourced Converters in Power Systems:Modeling, Control, and Applications, IEEE, 2010.

[53] J. Liu, Y. Miura, H. Bevrani, T. Ise, Enhanced virtual synchronous generator control for parallel inverters in microgrids, IEEE Transactions on Smart Grid 8 (2017) 2268–2277. doi:10.1109/TSG.2016.2521405.

[54] T. Shintai, Y. Miura, T. Ise, Reactive power control for load sharing with virtual synchronous generator control, in: Proceedings of The 7th International Power Electronics and Motion Control Conference, volume 2, 2012, pp. 846–853. doi:10.1109/IPEMC.2012.6258956.

[55] J. Alipoor, Y. Miura, T. Ise, Stability assessment and optimization methods for microgrid with multiple vsg units, IEEE Transactions on Smart Grid 9 (2018) 1462–1471. doi:10.1109/TSG.2016.2592508.

[56] J. Alipoor, Y. Miura, T. Ise, Power system stabilization using virtual synchronous generator with alternating moment of inertia, IEEE Journal of Emerging and Selected Topics in Power Electronics 3 (2015) 451–458. doi:10.1109/JESTPE.2014.2362530.

[57] J. Alipoor and Y. Miura and T. Ise, Voltage sag ride-through performance of virtual synchronous generator, in: 2014 International Power Electronics Conference (IPEC-Hiroshima 2014 - ECCE ASIA), 2014, pp. 3298–3305. doi:10.1109/IPEC.2014.6870160.

[58] National Grid, THE GRID CODE, 39, National Grid, 2020. URL: https://www.nationalgrideso.com/document/162271/download, [Accessed on 19-Feb-2020].

[59] M. Yu, A. J. Roscoe, C. D. Booth, A. Dysko, R. Ierna, J. Zhu, N. Grid, H. Urdal, Use of an inertia-less virtual synchronous machine within future power networks with high penetrations of converters, in: 2016 Power Systems Computation Conference, 2016, pp. 1–7. doi:10.1109/PSCC.2016.7540926.

[60] L. R. Castillo, A. Roscoe, Experimental validation of a novel inertia-less vsm algorithm, in: 2018 IEEE Power Energy Society Innovative Smart Grid Technologies Conference (ISGT), 2018, pp. 1–5. doi:10.1109/ISGT.2018.8403384.

[61] A. J Roscoe, M. Yu, A. Dyśko, C. Booth, R. Ierna, J. Zhu, H. Urdal, A vsm (virtual synchronous machine) convertor control model suitable for rms studies for resolving system operator / owner challenges, 15th Wind Integration Workshop (2016). URL: http://strathprints.strath.ac.uk/58053/.

[62] K. S. Yuko Hirase, Kazuhiro Abe, Y. Shindo, A grid-connected inverter with virtual synchronous generator model of algebraic type, IEEJ Transactions on Power and Energy 132 (2012) 371–380. doi:https://doi.org/10.1541/ieejpes.132.371.

[63] L. Zhang, L. Harnefors, H. Nee, Power-Synchronization Control of Grid-Connected Voltage-Source Converters, IEEE Transactions on Power Systems 25 (2010) 809–820. doi:10.1109/TPWRS.2009.2032231.

[64] M. Ashabani, Y. A. R. I. Mohamed, M. Mirsalim, M. Aghashabani, Multivariable droop control of synchronous current converters in weak grids/microgrids with decoupled dq-axes currents, IEEE Transactions on Smart Grid 6 (2015) 1610–1620. doi:10.1109/TSG.2015.2392373.

[65] L. Zhang, L. Harnefors, H. Nee, Interconnection of Two Very Weak AC Systems by VSC-HVDC Links Using Power-Synchronization Control, IEEE Transactions on Power Systems 26 (2011) 344–355. doi:10.1109/TPWRS.2010.2047875.

[66] L. Zhang, L. Harnefor, H. Nee, Modeling and Control of VSC-HVDC Links Connected to Island Systems, IEEE Transactions on Power Systems 26 (2011) 783–793. doi:10.1109/TPWRS.2010.2070085.

[67] W. Zhang, A. M. Cantarellas, J. Rocabert, A. Luna, P. Rodriguez, Synchronous power controller with flexible droop characteristics for renewable power generation systems, IEEE Transactions on Sustainable Energy 7 (2016) 1572–1582. doi:10.1109/TSTE.2016.2565059.

[68] W. Zhang, D. Remon, P. Rodriguez, Frequency support characteristics of grid-interactive power converters based on the synchronous power controller, IET Renewable Power Generation 11 (2017) 470–479. doi:10.1049/iet-rpg.2016.0557.

[69] S. S. Thale, V. Agarwal, Controller area network assisted grid synchronization of a microgrid with renewable energy sources and storage, IEEE Transactions on Smart Grid 7 (2016) 1442–1452. doi:10.1109/TSG.2015.2453157.

[70] D. Shi, Y. Luo, R. K. Sharma, Active synchronization control for microgrid reconnection after islanding, in: IEEE PES Innovative Smart Grid Technologies, Europe, 2014, pp. 1–6. doi:10.1109/ISGTEurope.2014.7028802.

[71] C. Verdugo, J. I. Candela, P. Rodriguez, Re-synchronization strategy for the synchronous power controller in hvdc systems, in: 2017 IEEE Energy Conversion Congress and Exposition (ECCE), 2017, pp. 5186–5191. doi:10.1109/ECCE.2017.8096872.

[72] M. Ashabani, J. Jung, Synchronous voltage controllers: Voltage-based emulation of synchronous machines for the integration of renewable energy sources, IEEE Access 8 (2020) 49497–49508. doi:10.1109/ACCESS.2020.2976892.

[73] M. Fazeli, P. Holland, Universal and seamless control of distributed resources-energy storage for all operational scenarios of microgrids, IEEE Transactions on Energy Conversion 32 (2017) 963–973. doi:10.1109/TEC.2017.2689505.

[74] M. Ashabani, F. D. Freijedo, S. Golestan, J. M. Guerrero, Inducverters: Pll-less converters with auto-synchronization and emulated inertia capability, IEEE Transactions on Smart Grid 7 (2016) 1660–1674. doi:10.1109/TSG.2015.2468600.

[75] E. Hossain, R. Perez, A. Nasiri, S. Padmanaban, A comprehensive review on constant power loads compensation techniques, IEEE Access 6 (2018) 33285–33305. doi:10.1109/ACCESS.2018.2849065.

[76] M. P. N. van Wesenbeeck, S. W. H. de Haan, P. Varela, K. Visscher, Grid-tied converter with virtual kinetic storage, in: 2009 IEEE Bucharest PowerTech, 2009, pp. 1–7. doi:10.1109/PTC.2009.5282048.

[77] J. Driesen, K. Visscher, Virtual synchronous generators, in: 2008 IEEE Power and Energy Society General Meeting - Conversion and Delivery of Electrical Energy in the 21st Century, 2008, pp. 1–3. doi:10.1109/PES.2008.4596800.

[78] K. Visscher, S. W. H. De Haan, Virtual synchronous machines (VSG's) for frequency stabilisation in future grids with a significant share of decentralized generation, in: CIRED Seminar 2008: SmartGrids for Distribution, 2008, pp. 1–4.

[79] V. Karapanos, S. de Haan, K. Zwetsloot, Real time simulation of a power system with vsg hardware in the loop, in: IECON 2011 - 37th Annual Conference of the IEEE Industrial Electronics Society, 2011, pp. 3748–3754. doi:10.1109/IECON.2011.6119919.

[80] V. Van Thong, A. Woyte, M. Albu, M. Van Hest, J. Bozelie, J. Diaz, T. Loix, D. Stanculescu, K. Visscher, Virtual synchronous generator: Laboratory scale results and field demonstration, in: 2009 IEEE Bucharest PowerTech, 2009, pp. 1–6. doi:10.1109/PTC.2009.5281790.

[81] V. Karapanos, Z. Yuan, S. de Haan, K. Visscher, A control algorithm for the coordination of multiple virtual sychnronous generator units, in: A. Apostolov (Ed.), Proceedings of the IEEE Powertech Conference, 2011, IEEE Society, 2011, pp. 1–7.

[82] B. Muftau, M. Fazeli, A. Egwebe, Stability analysis of a PMSG based Virtual Synchronous Machine, Electric Power Systems Research 180 (2020) 106170. URL: http://www.sciencedirect.com/science/article/pii/S0378779619304894. doi:https://doi.org/10.1016/j.epsr.2019.106170.

[83] Q. Zhong, Y. Zeng, Universal droop control of inverters with different types of output impedance, IEEE Access 4 (2016) 702–712. doi:10.1109/ACCESS.2016.2526616.

[84] N. Nasser, M. Fazeli, Buffered-microgrid structure for future power networks; a seamless microgrid control, IEEE Transactions on Smart Grid (2020). doi:10.1109/TSG.2020.3015573.

[85] M. O. Baruwa, M. Fazeli, Impact of virtual synchronous machines on low-frequency oscillations in power systems, IEEE Transactions on Power Systems (2020). doi:10.1109/TPWRS.2020.3029111.

[86] National Grid, Stability pathfinder RFI – Technical performanceand assessment criteria (Attachment 1), National Grid Warwick Technology Park, Gallows Hill, Warwick, UK., 2020. URL: https://www.nationalgrideso.com/news/carbon-free-system-stability-pathfinder-stakeholder-feedback-request, [Accessed on 11-Nov-2020].

[87] T. Prevost, G. Denis, WP3 - Control and Operation of a Grid with 100 % Converter-BasedDevices, MIGRATE, 2019. URL: https://www.h2020-migrate.eu/_Resources/Persistent/1bb0f89024e41a85bf94f1ec7ee6f8d7c34bc29a/D3.6-Requirementguidelinesforoperatingagridwith100powerelectronicdevices.pdf, [Accessed on 02-Oct-2020].

[88] P. M. Anderson, A. A. Fouad, Power System Control and Stability, IEEE, 2003.

[89] A. Delavari, I. Kamwa, P. Brunelle, Simscape power systems benchmarks for education and research in power grid dynamics and control, in: 2018 IEEE Canadian Conference on Electrical Computer Engineering (CCECE), 2018, pp. 1–5. doi:10.1109/CCECE.2018.8447645.

[90] C. Canizares, et al., Benchmark models for the analysis and control of small-signal oscillatory dynamics in power systems, IEEE Transactions on Power Systems 32 (2017) 715–722.

[91] H. Wen, M. Fazeli, A low-voltage ride-through strategy using mixed potential function for three-phase grid-connected PV systems, Electric Power Systems Research 173 (2019) 271 – 280. doi:https://doi.org/10.1016/j.epsr.2019.04.039.

[92] National Grid, System Operability Framework: Whole system Short Circuit Level, National Grid Warwick Technology Park, Gallows Hill, Warwick, UK., 2020. URL: https://www.nationalgrideso.com/research-publications/system-operability-framework-sof, [Accessed on 11-Nov-2020].

[93] R. A. Allah, Correlation-based synchro-check relay for power systems, IET Generation, Transmission Distribution 12 (2018) 1109–1120.

[94] M. J. Thompson, A. Li, R. Luo, M. C. Tu, I. Urdaneta, Advanced synchronizing systems for offshore power systems: Improving system reliability and flexibility, IEEE Industry Applications Magazine 23 (2017) 60–69. doi:10.1109/MIAS.2016.2600742.

[95] L. Fan, Modeling Type-4 Wind in Weak Grids, IEEE Transactions on Sustainable Energy 10 (2019) 853–864. doi:10.1109/TSTE.2018.2849849.

[96] R. Shi, X. Zhang, C. Hu, H. Xu, J. Gu, W. Cao, Self-tuning virtual synchronous generator control for improving frequency stability in autonomous photovoltaic-diesel microgrids, Journal of Modern Power Systems and Clean Energy 6 (2018) 482–494.

[97] National Grid, Black Start from Non-Traditional Generation Technologies, National Grid Warwick Technology Park, Gallows Hill, Warwick, UK., 2019. URL: https://www.nationalgrideso.com/document/148201/download, [Accessed on 14-Nov-2020].

[98] H. Alrajhi Alsiraji, R. El-Shatshat, Comprehensive assessment of virtual synchronous machine based voltage source converter controllers, IET Generation, Transmission Distribution 11 (2017) 1762–1769. doi:10.1049/iet-gtd.2016.1423.

[99] P. Kundur, N. Balu, M. Lauby, Power System Stability and Control, McGraw-Hill Education, 1994.

[100] Q. Peng, Q. Jiang, Y. Yang, T. Liu, H. Wang, F. Blaabjerg, On the stability of power electronics-dominated systems: Challenges and potential solutions, IEEE Transactions on Industry Applications 55 (2019) 7657–7670. doi:10.1109/TIA.2019.2936788.

[101] S. Peyghami, P. Davari, M. Fotuhi-Firuzabad, F. Blaabjerg, Standard test systems for modern power system analysis: An overview, IEEE Industrial Electronics Magazine 13 (2019) 86–105. doi:10.1109/MIE.2019.2942376.

[102] J. Machowski, Z. Lubosny, J. Bialek, J. Bumby, Power System Dynamics: Stability and Control, Wiley, 2020.

[103] J. Zhu, J. Hu, W. Hung, C. Wang, X. Zhang, S. Bu, Q. Li, H. Urdal, C. D. Booth, Synthetic inertia control strategy for doubly fed induction generator wind turbine generators using lithium-ion supercapacitors, IEEE Transactions on Energy Conversion 33 (2018) 773–783. doi:10.1109/TEC.2017.2764089.

[104] F. Katiraei, M. R. Iravani, P. W. Lehn, Small-signal dynamic model of a micro-grid including conventional and electronically interfaced distributed resources, IET Generation, Transmission Distribution 1 (2007) 369–378. doi:10.1049/iet-gtd:20045207.

[105] N. Pogaku, M. Prodanovic, T. C. Green, Modeling, analysis and testing of autonomous operation of an inverter-based microgrid, IEEE Transactions on Power Electronics 22 (2007) 613–625. doi:10.1109/TPEL.2006.890003.

[106] Y. Levron, J. Belikov, D. Baimel, A tutorial on dynamics and control of power systems with distributed and renewable energy sources based on the DQ0 transformation, Applied Sciences 8 (2018).

[107] J. Belikov, Y. Levron, Uses and misuses of quasi-static time-varying phasor models in power systems, IEEE Transactions on Power Delivery 33 (2018) 3263–3266. doi:10.1109/TPWRD.2018.2852950.

[108] A. Bokhari et al, Experimental Determination of the ZIP Coefficients for Modern Residential, Commercial, and Industrial Loads, IEEE Transactions on Power Delivery 29 (2014) 1372–1381. doi:10.1109/TPWRD.2013.2285096.

[109] S. Rahnama, T. Green, C. H. Lyhne, J. D. Bendtsen, Industrial demand management providing ancillary services to the distribution grid: Experimental verification, IEEE Transactions on Control Systems Technology 25 (2017) 485–495. doi:10.1109/TCST.2016.2563385.

[110] A. Mileva, J. Johnston, J. H. Nelson, D. M. Kammen, Power system balancing for deep decarbonization of the electricity sector, Applied Energy 162 (2016) 1001 – 1009. URL: http://www.sciencedirect.com/science/article/pii/S0306261915014300. doi:https://doi.org/10.1016/j.apenergy.2015.10.180.

[111] Z. A. Khan, D. Jayaweera, Smart meter data based load forecasting and demand side management in distribution networks with embedded pv systems, IEEE Access 8 (2020) 2631–2644. doi:10.1109/ACCESS.2019.2962150.

[112] P. Palensky, D. Dietrich, Demand side management: Demand response, intelligent energy systems, and smart loads, IEEE Transactions on Industrial Informatics 7 (2011) 381–388. doi:10.1109/TII.2011.2158841.

[113] A. Ipakchi, F. Albuyeh, Grid of the future, IEEE Power and Energy Magazine 7 (2009) 52–62. doi:10.1109/MPE.2008.931384.

[114] A. Q. Huang, M. L. Crow, G. T. Heydt, J. P. Zheng, S. J. Dale, The future renewable electric energy delivery and management (freedm) system: The energy internet, Proceedings of the IEEE 99 (2011) 133–148. doi:10.1109/JPROC.2010.2081330.

[115] National Grid Electricity System Operator, Demand Side Flexibility Annual Report 2019, National Grid, 2019. URL: https://www.powerresponsive.com/wp-content/uploads/2020, [Accessed on 5-Nov-2020].

[116] National Grid Electricity System Operator, A short guide to how your business can profit from Demand Side Response, National Grid, 2018. URL: https://www.powerresponsive.com/wp-content/uploads/2019, [Accessed on 5-Nov-2020].

[117] B. Foster, T. Bialecki, D. Burns, D. Kathan, M. P. Lee, S. Peirovi, 2019 Assessment of Demand Response and Advanced Metering, Federal Energy Regulatory Commission, 2019. URL: https://www.ferc.gov/sites/default/files/2020-04/DR-AM-Report2019_2.pdf, [Accessed on 02-Oct-2020].

[118] A. Chase, R. Gross, P. Heptonstall, M. Jansen, M. Kenefick, B. Parrish, P. Robson, REALISING THE POTENTIAL OF DEMAND-SIDE RESPONSE TO 2025, Departmant for Business, Energy & Industrial Strategy, 2017. URL: https://assets.publishing.service.gov.uk/government/uploads/system/uploads/attachment_data/file/657144/DSR_Summary_Report.pdf, [Accessed on 26-Nov-2020].

[119] G. Schuitema, L. Ryan, C. Aravena, The consumer's role in flexible energy systems: An interdisciplinary approach to changing consumers' behavior, IEEE Power and Energy Magazine 15 (2017) 53–60. doi:10.1109/MPE.2016.2620658.

[120] F. Wilches-Bernal, R. H. Byrne, J. Lian, Damping of Inter-Area Oscillations via Modulation of Aggregated Loads, IEEE Transactions on Power Systems 35 (2020) 2024–2036. doi:10.1109/TPWRS.2019.2948116.

[121] C. Zhang, D. Ke, Y. Sun, C. Y. Chung, J. Xu, Investigations of Large-Scale Voltage-Dependent Loads for Damping Inter-Area Oscillations: Mechanism and Robust Decentralized Control, IEEE Transactions on Power Systems 33 (2018) 6037–6048. doi:10.1109/TPWRS.2018.2854648.

[122] M. Monfared, M. Fazeli, R. Lewis, J. Searle, Fuzzy predictor with additive learning for very short-term pv power generation, IEEE Access 7 (2019) 91183–91192. doi:10.1109/ACCESS.2019.2927804.

[123] National Grid, Operability Impact of Distributed Storage and Electric Vehicles, National Grid, 2020. URL: https://www.nationalgrideso.com/document/166736/download, [Accessed on 06-Oct-2020].

[124] M. Stewart, Future Energy Scenarios, National Grid Warwick Technology Park, Gallows Hill, Warwick, UK., 2017. URL: https://investors.nationalgrid.com/~/media/Files/N/National-Grid-IR-V2/reports/2016-17/fes-2017-final.pdf, [Accessed on 26-Nov-2020].

[125] F. Slye, Future Energy Scenarios, National Grid Warwick Technology Park, Gallows Hill, Warwick, UK., 2019. URL: https://www.nationalgrideso.com/sites/eso/files/documents/fes-2019.pdf, [Accessed on 26-Nov-2020].

[126] C. Liu, K. T. Chau, D. Wu, S. Gao, Opportunities and Challenges of Vehicle-to-Home, Vehicle-to-Vehicle, and Vehicle-to-Grid Technologies, Proceedings of the IEEE 101 (2013) 2409–2427. doi:10.1109/JPROC.2013.2271951.

[127] M. Rezkalla, A. Zecchino, S. Martinenas, A. M. Prostejovsky, M. Marinelli, Comparison between synthetic inertia and fast frequency containment control based on single phase EVs in a microgrid, Applied Energy 210 (2018) 764 – 775. doi:https://doi.org/10.1016/j.apenergy.2017.06.051.

[128] Y. Ding, P. Nyeng, J. Østergaard, M. D. Trong, S. Pineda, K. Kok, G. B. Huitema, O. S. Grande, Ecogrid EU - a large scale smart grids demonstration of real time market-based integration of numerous small DER and DR, in: 2012 3rd IEEE PES Innovative Smart Grid Technologies Europe (ISGT Europe), 2012, pp. 1–7. doi:10.1109/ISGTEurope.2012.6465895.

[129] J. Wang, S. You, Y. Zong, C. Træholt, Energylab nordhavn: An integrated community energy system towards green heating and e-mobility, in: 2017 IEEE Transportation Electrification Conference and Expo, Asia-Pacific (ITEC Asia-Pacific), 2017, pp. 1–6. doi:10.1109/ITEC-AP.2017.8080846.

[130] G. Zuckeru, F. Kupzog, D. Reiter, Smart Grids Strategy for Salzburg, Austria, in: 21st International Conference on Electricity Distribution, 2011, pp. 1–5.

[131] U. Markovic, O. Stanojev, P. Aristidou, G. Hug, Partial grid forming concept for 100% inverter-based transmission systems, in: 2018 IEEE Power Energy Society General Meeting (PESGM), 2018, pp. 1–5. doi:10.1109/PESGM.2018.8586114.

[132] Q. Zhong, Power-electronics-enabled autonomous power systems: Architecture and technical routes, IEEE Transactions on Industrial Electronics 64 (2017) 5907–5918. doi:10.1109/TIE.2017.2677339.

[133] Q. Zhong, Virtual synchronous machines: A unified interface for grid integration, IEEE Power Electronics Magazine 3 (2016) 18–27. doi:10.1109/MPEL.2016.2614906.

[134] J. Li, H. You, J. Qi, M. Kong, S. Zhang, H. Zhang, Stratified optimization strategy used for restoration with photovoltaic-battery energy storage systems as black-start resources, IEEE Access 7 (2019) 127339–127352. doi:10.1109/ACCESS.2019.2937833.

[135] K. M. J. Rahman, M. M. Munnee, S. Khan, Largest blackouts around the world: Trends and data analyses, in: 2016 IEEE International WIE Conference on Electrical and Computer Engineering (WIECON-ECE), 2016, pp. 155–159. doi:10.1109/WIECON-ECE.2016.8009108.

[136] G. Patsakis, D. Rajan, I. Aravena, J. Rios, S. Oren, Optimal black start allocation for power system restoration, IEEE Transactions on Power Systems 33 (2018) 6766–6776. doi:10.1109/TPWRS.2018.2839610.

[137] Chunyan Li, Yuanzhang Sun, Xiangyi Chen, Analysis of the blackout in europe on november 4, 2006, in: 2007 International Power Engineering Conference (IPEC 2007), 2007, pp. 939–944.

[138] European Network of Transmission System Operators for Electricity, POWER EUROPE FACTS 2019, 2018. URL: https://eepublicdownloads.entsoe.eu/clean-documents/Publications/ENTSO-E%20general%20publications/ENTSO-E_PowerFacts_2019.pdf, [Accessed on 14-Nov-2020].

[139] National Grid, Black Start from Distributed Energy Resources, National Grid Warwick Technology Park, Gallows Hill, Warwick, UK., 2018. URL: https://www.ofgem.gov.uk/ofgem-publications/143706, [Accessed on 14-Nov-2020].

[140] A. Alassi, K. Ahmed, A. Egea-Alvarez, O. Ellabban, Performance evaluation of four grid-forming control techniques with soft black-start capabilities, in: 2020 9th International Conference on Renewable Energy Research and Application (ICRERA), 2020, pp. 221–226. doi:10.1109/ICRERA49962.2020.9242758.

[141] A. Asheibi, S. Shuaib, A case study on black start capability assessment, in: 2019 International Conference on Electrical Engineering Research Practice (ICEERP), 2019, pp. 1–5. doi:10.1109/ICEERP49088.2019.8956978.

[142] Xavier Potau and Samuel Leistner and George Morrison, Battery Promoting Policies in Selected Member States, 2018. URL: https://ec.europa.eu/energy/sites/ener/files/policy_analysis_-_battery_promoting_policies_in_selected_member_states.pdf, [Accessed on 14-Nov-2020].

[143] S. Van Broekhoven, N. Judson, J. Galvin, J. Marqusee, Leading the charge: Microgrids for domestic military installations, IEEE Power and Energy Magazine 11 (2013) 40–45. doi:10.1109/MPE.2013.2258280.